Faculdade de Engenharia da Universidade do Porto
Instituto de Ciências Biomédicas Abel Salazar

Antimicrobial Nanoparticles to Fight Bacterial Wound Infections

António Miguel Valente Braz Sepúlveda Ramôa

Dissertação realizada no âmbito do
Mestrado Integrado em Bioengenharia (Biotecnologia Molecular)

Orientador: Cláudia Monteiro, PhD
I3S – Instituto de Investigação e Inovação em Saúde, Universidade do Porto, Bioengineered Surfaces Group
INEB – Instituto de Engenharia Biomédica, Porto, Portugal
Coorientador: Cristina Martins, PhD
I3S – Instituto de Investigação e Inovação em Saúde, Universidade do Porto, Bioengineered Surfaces Group
INEB – Instituto de Engenharia Biomédica, Porto, Portugal
ICBAS – Instituto de Ciências Biomédicas Abel Salazar, Universidade do Porto, Porto, Portugal

Setembro de 2021

Resumo

As infeções de feridas crónicas representam um grande desafio na medicina moderna e a sua prevalência deverá aumentar nos próximos anos devido ao aumento da esperança de vida e da incidência de comorbilidades como a obesidade e a diabetes. A colonização por bactérias tem um papel importante nestas feridas, sendo *Staphylococcus aureus* e *Pseudomonas aeruginosa* as duas espécies mais frequentemente isoladas. Estas infeções ocorrem frequentemente sob a forma de biofilme, levando a uma diminuição da eficácia dos tratamentos. Tendo em conta a atual crise de resistência a antibióticos, bem como a toxicidade e baixa eficácia dos desinfetantes tópicos utilizados, há uma necessidade urgente de novos tratamentos antimicrobianos.

Os péptidos antimicrobianos (AMPs) são moléculas universais de largo espetro com propriedades antimicrobianas, imunomoduladoras e de cicatrização de feridas, que têm ganho destaque como possíveis tratamentos antimicrobianos devido à sua elevada eficácia e baixa probabilidade de induzir resistência. A conjugação com nanopartículas (NPs) é uma das possíveis estratégias para melhorar a estabilidade e biocompatibilidade dos AMPs.

Este trabalho avaliou a atividade antimicrobiana de MSI-78(4-20), um AMP potente derivado de *pexiganan*, quando imobilizado em NPs compostas de poli(ácido lático-co-glicólico)-polietilenoglicol (PLGA-PEG) e PLGA-PEG-maleimida (PLGA-PEG-Mal) através de uma reação maleimida-tiol.

As AMP-NPs obtidas têm uma morfologia esférica, um tamanho de cerca de 100 nm e apresentam baixa polidispersão. Além disso, apresentam uma carga superficial aumentada quando comparadas com NPs não modificadas (PLGA-PEG) devido à presença de AMP catiónico. Análise por espetroscopia de infravermelho (FTIR) revelou os picos característicos de PLGA-PEG e AMP, e ressonância magnética nuclear (NMR) mostrou uma diminuição significativa do pico da Mal, confirmando a ligação covalente.

Em comparação com o AMP livre, a atividade antimicrobiana das AMP-NPs em meio de crescimento foi mantida para *S. aureus,* mas diminuiu ligeiramente para *P. aeruginosa*. A atividade em fluido simulado da ferida foi semelhante àquela em meio de crescimento para *S. aureus*, mas houve perda de atividade evidente para *P. aeruginosa*. A cinética de morte do AMP foi melhorada em ambas as estirpes após imobilização nas NPs, e resultados preliminares da atividade antibiofilme sugerem que NPs de PLGA-PEG são mais eficazes na inibição do crescimento de biofilme do que AMP-NPs.

Em geral, estes resultados indicam que esta formulação é um candidato promissor para o desenvolvimento de tratamentos eficazes para infeções de feridas crónicas com base em AMPs.

Abstract

Chronic wound infections pose a great challenge in modern medicine and are likely to increase in prevalence due to the rise in life expectancy and increased incidence of comorbidities such as obesity and diabetes. Bacterial colonization plays a major role in these wounds, with *Staphylococcus aureus* and *Pseudomonas aeruginosa* being the two most commonly isolated pathogens. These infections frequently occur in the form of biofilm, leading to decreased treatment efficacy. In the wake of the current antibiotic resistance crisis as well as the toxicity and low effectiveness of topical disinfectants, there is an urgent need for new antimicrobial treatments.

Antimicrobial peptides (AMPs) are ubiquitous broad-spectrum agents with antimicrobial, immunomodulatory and wound healing properties, which have gained recent attention as possible antimicrobial treatments due to high effectiveness and low likelihood of inducing resistance. Conjugation with nanoparticles (NPs) is a possible strategy to improve AMP stability and biocompatibility.

This work assessed the antimicrobial activity of MSI-78(4-20), a potent AMP derived from pexiganan, when immobilized on NPs composed of poly(lactide-co-glycolide acid)-polyethylene glycol (PLGA-PEG) and PLGA-PEG-maleimide (PLGA-PEG-Mal) through maleimide-thiol chemistry.

The obtained AMP-NPs had a spherical morphology, a size around 100 nm and presented low polydispersity. Also, AMP-NPs displayed an increased surface charge when compared to bare NPs, conferred by the cationic AMP. Fourier-transform infrared spectroscopy (FTIR) showed the characteristic peaks of PLGA-PEG and AMP and nuclear magnetic resonance (NMR) displayed a significant decrease of the Mal peak, confirming covalent tethering.

Compared to free AMP, antimicrobial activity of AMP-NPs in growth medium was maintained for *S. aureus* but decreased slightly for *P. aeruginosa*. AMP-NP activity in simulated wound fluid (SWF) was similar to that in growth medium for *S. aureus* but loss of activity was evident for *P. aeruginosa*. AMP killing kinetics were improved in both strains upon NP immobilization and preliminary results of antibiofilm activity suggest bare PLGA-PEG NPs are more effective at inhibiting biofilm formation than AMP-NPs.

Overall, our results indicate that this AMP-NP formulation is a promising candidate to develop effective treatments for chronic wound infections based on AMPs.

Agradecimentos

No fim desta enriquecedora etapa, quero começar por agradecer às minhas orientadoras. À Cláudia Monteiro, pela sua constante disponibilidade e motivação, bem como por alimentar o meu espírito crítico e interpretação científica, e à Cristina Martins pela sua orientação e voto de confiança ao integrar este grupo.

De seguida, a todos os elementos que fizeram ou fazem parte do grupo Bioengineered Surfaces, pela sua companhia, amizade e ajuda durante o período de integração no laboratório e todo o restante percurso, em especial ao Luís Moreira, Ana Rita Pinto, Pedro Alves, Bruna Costa, Diana Fonseca, Duarte Moura e Helena Ferreira.

Também agradeço aos restantes que contribuíram de alguma forma para este trabalho, nomeadamente à Cátia Teixeira, Victoria Leiro, Paula Gomes, José das Neves, Ana Rita Pinto, Cecília Durães e Rui Fernandes, assim como ao Ricardo Vidal pelo conhecimento teórico e experimental que me transmitiu.

Agradeço aos meus colegas cujos percursos académicos pude acompanhar, pela troca de ideias e companheirismo, bem como aos amigos que sempre me apoiaram e mostraram interesse no meu trabalho mesmo pertencendo a noutras áreas.

Por fim, agradeço aos meus pais e irmãs pelo constante apoio e confiança durante todos os desafios do dia-a-dia destes últimos anos, e a toda a minha família, por nunca duvidarem de mim.

Este trabalho teve o apoio financeiro do projeto AntINFECT: *Bioengineered Advanced Therapies for Problematic Infected Wounds* (POCI-01-0145-FEDER- 031781) e da Fundação para a Ciência e a Tecnologia (FCT) (UIDB/50006/2020).

Index

Figures list

Tables list

Abbreviations and symbols

^{1}H-NMR	Proton nuclear magnetic resonance
AgNPs	Silver nanoparticles
Ahx	6-aminohexanoic acid
AMP	Antimicrobial peptide
AMP-NPs	Antimicrobial peptide nanoparticles
AMR	Antimicrobial resistance
APCs	Antigen-presenting cells
Ara4N	4-Aminoarabinose
AuNPs	Gold nanoparticles
BGC	Biofilm growth check
BLP	Bacterial lipoprotein
BSA	Bovine serum albumin
CFUs	Colony forming units
Chit	Chitosan
Cys	Cysteine
DAMPs	Damage-associated molecular patterns
DFU	Diabetic foot ulcer
DLS	Dynamic light scattering
DMPC	1,2-dimyristoyl-sn-glycero-phosphocholine
DMSO	Dimethyl sulfoxide
ECM	Extracellular matrix
EGFR	Epidermal growth factor receptor
EPM	Electrophoretic mobility
EPR	Enhanced permeation and retention
EPS	Extracellular polymeric substance
FBS	Fetal bovine serum
FGF	Fibroblast growth factor
FTIR	Fourier-transform infrared
GA	Glycolic acid
GLASS	Global Antimicrobial Resistance and Use Surveillance System
HBOT	Hyperbaric oxygen therapy
HDPs	Host defense peptides
IE	Immobilization efficiency

IL-1	Interleukin-1
LA	Lactic acid
LPS	Lipopolysaccharide
Mal	Maleimide
MBC	Minimum bactericidal concentration
MBEC	Minimum biofilm eradication concentration
MDR	Multidrug-resistant
MHB	Mueller-Hinton broth
MIC	Minimum inhibitory concentration
MMPs	Matrix metalloproteinases
MNPs	Magnetic nanoparticles
MRSA	Methicillin-resistant *Staphylococcus aureus*
MSNs	Mesoporous silica nanoparticles
MSSA	Methicillin-sensitive *Staphylococcus aureus*
NETs	Neutrophil extracellular traps
NLCs	Nanostructured lipid carriers
NPs	Nanoparticles
NTA	Nanoparticle tracking analysis
PAMPs	Pathogen-associated molecular patterns
PBS	Phosphate-buffered saline
PdI	Polydispersity index
PEG	Polyethylene glycol
PLA	Polylactic acid
PLGA	Poly(lactic-co-glycolic acid)
POPC	1-palmitoyl-2-oleoyl-sn-glycero-3-phosphocholine
POPG	1-palmitoyl-2-oleoyl-sn-glycero-3-phosphoglycerol
PQS	*Pseudomonas* quinolone signal
PVL	Panton-Valentine leukocidin
QDs	Quantum dots
ROS	Reactive oxygen species
SC	Stratum corneum
SCV	Small colony variant
SLNs	Solid lipid nanoparticles
SPPS	Solid-phase peptide synthesis
SWF	Simulated wound fluid
TAs	Teichoic acids
TEM	Transmission electron microscopy
TNF-α	Tumor necrosis factor alpha
TSA	Tryptic soy agar
TSB	Tryptic soy broth

VEGF	Vascular endothelial growth factor
VRSA	Vancomycin-resistant *Staphylococcus aureus*
WHO	World Health Organization
XDR	Extensively drug-resistant

Symbols list

M_w	Molecular weight
OD	Optical density
PdI	Polydispersity Index
ZP	Zeta potential

Introduction

1. Chronic wounds

1.1. An overview of wound healing

The process of wound healing is essential to regain skin integrity and function after an injury (figure 1). It is a complex process that requires precise coordination of multiple cell types in a timely manner (Rutter, 2018). In acute wounds, it can be divided into five distinguishable but overlapping phases, summarized by (Rodrigues et al., 2019):

A. Hemostasis

Firstly, there is constriction of immediate blood vessels and platelet activation to form a blood clot, to achieve coagulation and hemostasis. Primary hemostasis occurs by platelet aggregation and plug formation, while secondary hemostasis involves activation of the coagulation cascade, in which soluble fibrinogen is converted to an insoluble fibrin mesh. Together, these two structures form the thrombus, which stops bleeding and serves as scaffold for the remaining phases of wound healing.

B. Inflammation

The inflammatory phase consists of the recruitment and differentiation of immune cells in the wound. Chemokines, elevated intracellular calcium levels, reactive oxygen species (ROS) gradient, damage-associated molecular patterns (DAMPs) and others act as signals for immune cell recruitment.

Neutrophils are the first line of defense against bacteria, releasing toxic granules, producing ROS, performing phagocytosis, and creating neutrophil extracellular traps (NETs). After neutrophil clearance, monocytes infiltrate the wound and originate tissue-activated macrophages. In their pro-inflammatory (M1) state, macrophages engulf and digest pathogens and secrete matrix metalloproteinases (MMPs) that degrade the thrombus. Inflammation is resolved with the transition of macrophages to their anti-inflammatory (M2) phenotype, which contributes to blood vessel formation, fibroblast differentiation and extracellular matrix (ECM) deposition.

In the later adaptive response, other cell types such as mast cells, Langerhans cells, dermal dendritic cells, and T cells are responsible for recognizing and eliminating specific antigens.

C. Growth

In this phase, fibroblasts differentiate into myofibroblasts, which deposit an ECM rich in collagen III and contract the wound, producing a granulation tissue which serves as scaffold for other

concurrent processes. Neovascularization, being the formation of new blood vessels, takes place to ensure delivery of oxygen and nutrients to the healing wound. In adults, this process is done mainly by angiogenesis, in which there is activation, proliferation and migration of local macrovascular endothelial cells in response to pro-angiogenic signals such as vascular endothelial growth factor (VEGF) and fibroblast growth factor (FGF). At the same time, pericytes from the basal lamina provide a scaffold for and surround the growing vessels.

D. Re-epithelialization

Here, keratinocytes of the wound edge lose their adhesions and migrate to close the gap in a structure named migrating epithelial tongue. Specific skin stem cell populations give rise to the hair follicles, sebaceous glands, and melanocytes, with the latter being responsible for the repigmentation of the epidermis.

E. Maturation and remodeling

This last step takes place after wound closure and is critical for restoration of skin function and aesthetics. There is regression of the neovasculature formed during angiogenesis to form more stable and supported blood vessels through a process called pruning, and reorganization of the ECM by MMPs, in which the collagen III of the granulation tissue is replaced by the stronger collagen I. In the post-natal setting, the remodeling phase restores the barrier function and approximate tensile strength of the skin but leaves a fibrotic scar in the wound site.

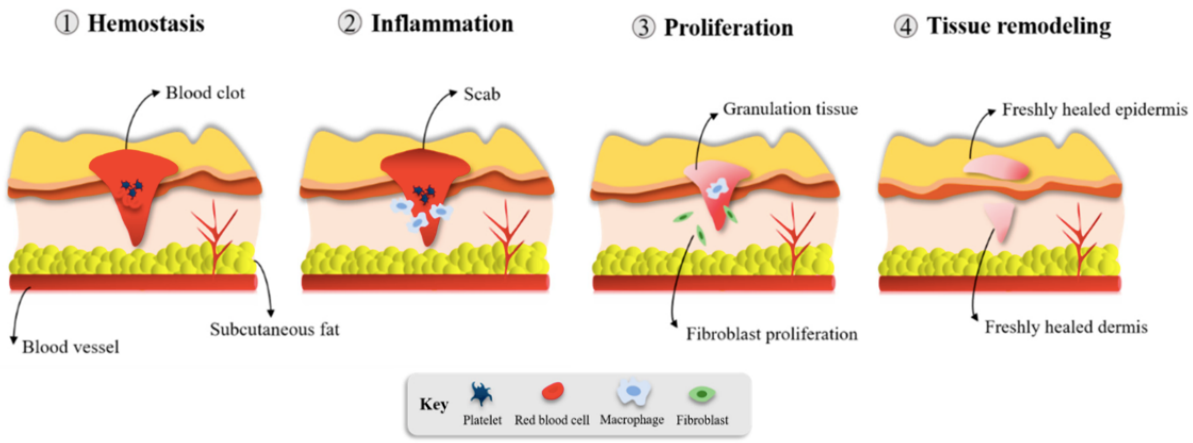

Figure 1 - Scheme of the normal process of wound healing. Phases C and D mentioned above are usually grouped in a common proliferation phase (Shajari et al., 2017).

1.2. Definition and classification

When the normal healing process is detained, acute wounds can become chronic or nonhealing wounds. By definition, chronic wounds “have failed to proceed through an orderly and timely process to produce anatomic and functional integrity, or proceeded through the repair process without establishing a sustained anatomic and functional result” (Lazarus et al., 1994). Although the time span necessary to define chronicity is not agreed upon, a wound is considered non-healing if it does

not heal usually between 4 weeks and 3 months (Järbrink et al., 2017). As such, medical intervention is often necessary to treat them.

The Wound Healing Society classifies chronic wounds into four classes: pressure ulcers, diabetic ulcers, venous ulcers and arterial insufficiency ulcers (Robson & Barbul, 2006). Pressure ulcers result from prolonged pressure to the skin and the underlying muscle and are common in people with reduced mobility and decreased sensory perception. Diabetic ulcers are typical in diabetic patients due to vascular impairment and deficiencies in muscle metabolism. Venous and arterial ulcers in the lower extremities can occur due to poor valve function and inadequate blood supply, respectively. Other types include wounds from infectious, ischemic, radiation-poisoning and surgical origin (woundcarecenters.org, n.d.).

1.3. Factors associated with chronic wounds

Often associated with chronic wounds are prolonged or excessive inflammation, persistent infection, biofilm formation, hypoxia and inadequate cell response to stimuli (Demidova-Rice et al., 2012). These can be inter-dependent and not only contribute to but also result from wound chronicity. Some of these aspects will be further discussed below.

1.3.1. Inflammation

Despite an intense inflammatory reaction being useful for highly contaminated wounds, it is detrimental for the repair of most wounds. Most chronic wounds get stuck in the inflammatory phase of wound healing, which is generally attributed to a disturbed balance between pro-inflammatory molecules and their inhibitors – unlike what is seen in acute wounds (Schultz & Mast, 1998). The major contributor appears to be excessive neutrophil infiltration with consequent over-production of ROS. While ROS damage cells and the extracellular matrix, secreted proteases degrade important growth factors involved in regeneration. Taken together, these mechanisms delay cell migration/proliferation and collagen synthesis taking place in the following proliferative phase. Factors associated with increased inflammation are ageing, hypoxia, ischemia-reperfusion injury, and bacterial colonization (Zhao et al., 2016).

1.3.2. Infection

Bacteria enter wounds as soon as the skin barrier is disrupted. Multiple stages can take place from this timepoint forward: the presence of non-replicating organisms is defined as contamination; colonization is the presence of replicating organisms without tissue damage; local infection or critical colonization is an intermediate step that marks the initial local tissue response; and finally invasive infection occurs when there is subsequent host injury (Edwards & Harding, 2004). Risk factors for infection include stress, malnutrition, poor blood flow, immune or metabolic disorders, old age, hospitalization, poor body build, concurrent infections, and administration of immunosuppressant drugs (Scanlon, 2005).

Bacteria themselves and secreted exotoxins can prolong the production of pro-inflammatory cytokines such as interleukin-1 (IL-1) and tumor necrosis factor-alpha (TNF-α), as well as attack various cell types and cause tissue necrosis (Ovington, 2003). During cell lysis, the endotoxins

lipopolysaccharide (LPS) and bacterial lipoprotein (BLP) in the outer membrane of Gram-negative bacteria can also affect VEGF signaling and endothelial cell proliferation (Power et al., 2001). This increases the levels of MMPs and decreases that of their inhibitors and growth factors, which translates to a prolonged or detained inflammatory phase of wound healing (Robson et al., 1990). However, this appears to be true only for infective levels of bacteria, as those below this threshold actually accelerate wound healing (Edwards & Harding, 2004; Laato et al., 1988).

In a microbiological wound analysis of 213 patients, the most commonly identified bacterial species in order of abundance were *Staphylococcus aureus* (*S. aureus*), *Pseudomonas aeruginosa* (*P. aeruginosa*), *Proteus mirabilis*, *Escherichia coli* and *Corynebacterium spp*. Besides being the most common isolates, chronic wounds frequently present co-infection by *S. aureus* and *P. aeruginosa* (Bessa et al., 2015). A similar study confirmed the prevalence of these species in venous leg ulcers, with *S. aureus* being present in 93.5 % of wounds and *P. aeruginosa* in 52.2 % (Gjødsbøl et al., 2006).

S. aureus and *P. aeruginosa* are facultatively aerobic bacteria part of the skin microbiota, the first being a Gram-positive round-shaped organism and the second a Gram-negative bacillus. Both are opportunistic pathogens that can cause mild infections in otherwise healthy people but can lead to serious and even life-threatening disease in immunocompromised patients. *S. aureus* is commonly known to cause bacteremia, endocarditis, and skin, osteoarticular, prosthetic device and pleuropulmonary infections. It can evade immune clearance by blocking leukocyte chemotaxis, sequestering host antibodies, preventing detection through capsule or biofilm, and resisting digestion after phagocytosis. Virulence factors found in this species include the Panton-Valentine leucocidin (PVL), alpha-hemolysin, and phenol-soluble modulins, all causing human cell lysis (Tong et al., 2015). In turn, *P. aeruginosa* can cause pneumonia (particularly in cystic fibrosis patients), endocarditis, meningitis and wound infections, and notable virulence factors are flagella, type IV pili, alkaline protease, elastase, LPS, phospholipase, exotoxin A, pyoverdine, pyochelin, pyocyanin and *Pseudomonas* quinolone signal (PQS) (Lee & Yoon, 2017).

1.3.3. Biofilm

Bacterial biofilms also pose a great challenge in chronic wound treatment. Biofilms are complex structures of bacterial colonies encased in a hydrated polysaccharide matrix, able to adhere to wound surfaces. These harbor the formation of complex communities and protect pathogens from environmental stress, immune cells and antimicrobial agents, making bacteria more resistant than their planktonic state (Rajpaul, 2015). Although polysaccharides are the main ECM component of biofilms, proteins, nucleic acids, lipids and other molecules are also included, collectively called extracellular polymeric substance (EPS) (Y. K. Wu et al., 2019).

Biofilm growth and maintenance is mediated through quorum sensing, a bacterial cell-cell signaling mechanism which allows gene regulation as a response to cell population density. The process starts with the initial attachment of bacteria to a surface and each other, followed by formation of microcolonies, biofilm maturation, and finally dispersal. The major steps of biofilm growth can be seen on figure 2. Research suggests this process can start as a response to different environmental cues and biofilm architecture is dependent on factors such as species and environmental conditions (Tolker-Nielsen, 2015).

P. aeruginosa is one of the species with most researched biofilm, as highlighted in a review by (Lee & Yoon, 2017). Attachment to surfaces is mediated by adhesins, type IV pili and LPS, and this bacterium forms a complex biofilm architecture which includes water channels and a mushroom morphology. In terms of attachment in the wound environment, bacterial adhesins have been

implicated in binding to serum proteins such as fibronectin (Henderson et al., 2011). Quorum sensing contributes greatly to biofilm maturation, in which bacteria become more resistant to environmental stress and antibiotics. The final detachment phase can occur in three mechanisms: sloughing and erosion, passive methods which involve detachment of large and small portions of biomass, respectively; and seed dispersal, when single cells or microcolonies are released from the center of the biofilm through ECM degradation. Among other signals, dispersal can be induced by nutrient, oxygen, or pH levels. Biofilm resistance to antibiotics can be mainly attributed to the physical barrier provided by the ECM, and to the presence of cells with slower metabolism or ceased growth.

A study involving 93 patients found that 60 % of chronic wounds contained biofilm, as opposed to only 6 % of acute wounds (James et al., 2008). A more recent systematic review revealed an even higher biofilm prevalence of 78.2 % (Malone et al., 2017). Overall, this denotes that most infections in chronic wounds exist in the form of biofilm. Regardless, infection by microorganisms (planktonic or sessile) contributes to inflammation and delayed healing (Guo & DiPietro, 2010). Furthermore, mature biofilm can disperse to other areas of the body and cause systemic infection.

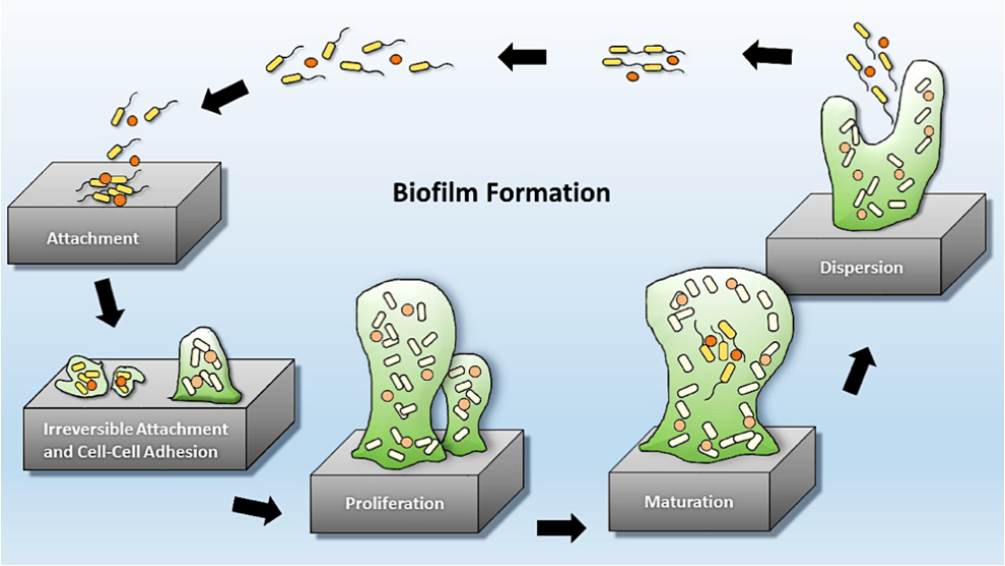

Figure 2 - The main steps of biofilm growth: attachment, irreversible attachment, proliferation, maturation, and dispersion (Perfectus Biomed Group, 2017).

1.4. Treatment

Wound treatment is one of the most ancient medical practices and has evolved considerably until current methods. The TIME guidelines were developed in 2003 by a group of experts in wound management to provide a systematic approach to treat nonhealing wounds, and contemplate four essential aspects of wound healing – tissue, infection, moisture imbalance, and edge advancement (Schultz et al., 2003).

At the tissue level, debridement consists of removing nonviable or necrotic tissue to facilitate healing. Surgical debridement is the traditional method of removing nonviable tissue using medical equipment while the patient is under anesthesia; mechanical debridement involves methods such as water irrigation and ultrasonography; autolytic debridement can be achieved by keeping wound moisture to allow digestion by endogenous enzymes; and less frequently, enzymatic or biologic

debridement is done by applying collagenase or placing maggots on the wound bed, which selectively digest nonviable tissue (Schultz et al., 2003).

To deal with infection, the first step is cleaning the wound with saline or tap water. Detergents, povidone-iodine, hydrogen peroxide, and acetic acid solutions are secondary due to inherent toxicity. The World Health Organization (WHO) recommends prophylaxis with systemic antibiotics for deep wounds and wounds at high risk of infection. Because the drug will not reach the source of infection, this needs to be combined with standard wound care. Topical antibiotics are not recommended due to the risk of developing resistance and allergic reactions (WHO, 2013). However, for superficially infected wounds, topical antibiotics are preferred to systemic antibiotics to limit development of bacterial resistance. Due to silver's established antimicrobial effect, silver dressings are recommended for a two-week trial for wounds either infected or at high risk of infection. Despite its efficacy, silver should be used with precaution as high concentrations are toxic to fibroblasts and could impair wound healing (Khansa et al., 2019). Medical-grade manuka honey also has efficacy against a great number of bacterial species. For patients with deep or systemic infections – on which the previous treatments provide no effect – systemic antibiotics are administered (Schultz et al., 2003).

Moisture balance is also an important parameter to control by using moisture-retentive dressings. The most common types are films, foams, hydrocolloids, alginates, and hydrogels. Finally, bioengineered dressings can be used to advance the wound edges by simulating the structure of human skin. These may include autografts from the patients' own cells or from animal cells (fibroblasts and keratinocytes) and skin components (such as collagen). Hyperbaric oxygen therapy (HBOT), which involves applying pure oxygen to wounds to prevent hypoxia, also has proof of effectiveness (Powers et al., 2016).

1.5. Impact

Wounds represent a considerable challenge in hospital care, as the global annual cost for wound care is expected to reach $3.5 B in 2021 and the wound-closure products market exceeding $15 B by 2022 (Sen, 2019). When it comes to chronic wounds, it is estimated that 1 % to 2 % of the population in developed countries will be affected in their lifetime (Nussbaum et al., 2018).

Because chronic wounds can stay open for a long period of time, they can cause significant pain, psychological stress, reduced mobility, and isolation (Walshe, 1995). When all treatment options have been attempted without success, an amputation must be performed. Epidemiological studies show that foot ulcers are the cause of 85 % of nontraumatic lower extremity amputations in patients with diabetes (Reiber et al., 1995). Unfortunately, this procedure is associated with a high risk of mortality. A cohort study of 1 053 diabetic patients found that mortality rates after 4 years were 65 % and 45 % for major and minor lower extremity amputation, respectively (Cascini et al., 2020).

The incidence of chronic wounds is expected to rise in the future due to an increase in life expectancy and a growing prevalence of comorbidities such as diabetes and obesity. Forecasts estimate that, between 2010 and 2030, the prevalence of obesity and severe obesity will increase by 33 % and 130 %, respectively (Finkelstein et al., 2012). Likewise, the number of people living with diabetes is expected to rise by 25 % from 2019 to 2030 (Saeedi et al., 2019). As such, more effective wound healing strategies will be needed to provide a faster resolution and prevent amputation and other extreme measures in the growing patient group.

2. Antimicrobial resistance

As mentioned, antibiotics are not currently advised for chronic wound treatment except in select cases. This is mainly due to the risk of bacteria in the wound developing resistance to the treatment. Additionally, there is the added possibility of applied antibiotics being ineffective due to the presence of resistant microorganisms in the wound. Together, these reasons explain why antibiotics are being discouraged in the modern medical setting.

The use of antibiotics at sublethal concentrations allows selection of resistance genes that can be transmitted by vertical inheritance or by horizontal gene transfer between species (Lerminiaux & Cameron, 2019). These genes translate into many possible mechanisms – efflux pumps, enzymatic degradation, modification of metabolic pathways, alteration of intracellular targets, and changes in membrane permeability.

The main driver of this phenomenon is the overuse of antibiotics in multiple sectors, namely human and animal use (particularly in the agricultural setting). This is aggravated by the fact that no major discoveries in the field of antibiotics have been made since the 1980s, in contrast with the fast evolution of antimicrobial resistance (AMR) (Christaki et al., 2020). As a result, infections have become harder to treat, medical costs have risen, hospital stays are prolonged, and mortality has increased.

A historic summary of the response to AMR has been made by (Podolsky, 2018). *S. aureus* was the first bacterial species to be described as resistant to penicillin. In the 1960s it was discovered that antibiotic resistance could also be transmitted horizontally, and there were reports of transmission from farm animals to humans. Concurrently, the first warnings were made of the risk of humanity returning to pre-antibiotic times. In 1976, Stuart Levy and colleagues stirred global concern with the "Statement Regarding Worldwide Antibiotic Misuse". Recently, AMR has started being viewed as a global emergency akin to climate change, in part due to forecasts of potential socioeconomic impact. In 2015, the WHO released the "Global Action Plan on Antimicrobial Resistance" and launched the Global Antimicrobial Resistance and Use Surveillance System (GLASS) to monitor the prevalence of resistant strains.

Among the drug-resistant bacteria that pose the greatest threat to human health are carbapenem-resistant *P. aeruginosa* and methicillin and vancomycin-resistant *S. aureus* (MRSA and VRSA, respectively) (Willyard, 2017). *P. aeruginosa* has a remarkable capacity of developing resistance in vivo, proven by the dissemination of multidrug-resistant (MDR) and extensively drug-resistant (XDR) *P. aeruginosa* (Horcajada et al., 2019) – in 2019, the European Center for Disease Prevention and Control reported that 3.4 % of isolates were resistant to all five antimicrobial groups tested (ECDC, 2020). As for *S. aureus*, MRSA was clinically identified in 1960 (10 years after the development of methicillin) and represented 42 % of clinical isolates in non-ICU patients in the USA from 1998 to 2003 (Lakhundi & Zhang, 2018; NNIS, 2003). In turn, VRSA was first reported in 2002 and is less frequent, with only 14 isolates in the USA as of 2015 arising from MRSA treatment with vancomycin (Shajari et al., 2017; Walters et al., 2015).

To get a scope on the current impact of the issue, it is estimated that around 33 000 people die every year due to antibiotic-resistant bacteria in the European Union (Cassini et al., 2019). If the current trends persist, in the future we could enter a post-antibiotic era, in which common diseases

and minor wounds could once again kill. In this scenario, predictions indicate a death toll of 10 million by the year 2050 (de Kraker et al., 2016). Because of this, the WHO has included AMR in the top 10 global public health threats facing humanity (WHO, 2020). Besides a better regulation of antibiotic use, one of the strategies to tackle AMR is the development of novel antimicrobial agents (WHO, 2017).

3. Antimicrobial peptides (AMPs)

3.1. Origin and structure

Antimicrobial peptides (AMPs) or host defense peptides (HDPs) are natural evolutionarily conserved molecules present in all living organisms which constitute one of the first lines of defense against invading pathogens. In mammals, AMPs are produced as part of the innate immune response by epithelial cells and phagocytes to combat pathogens that cross epithelial surfaces, and they can be organized into three main classes: defensins, cathelicidins and histatins. All human AMPs are produced by proteolytic processing from an inactive precursor (Otagiri et al., 2017). Some of these peptides are constitutively expressed, being stored in neutrophile granules and released at inflammation or infection sites, while others are expressed only in response to pathogen-associated molecular patterns (PAMPs) or cytokines. Amphibians, which live in highly contaminated environments, are a rich source of active peptides and the origin of a considerable portion of AMPs identified to date. These peptides are produced by cutaneous glands and released on the skin in case of anxiety, wounds, or electrical stimulation (Patocka et al., 2018). AMPs produced by bacteria – known as bacteriocins – have the purpose of competing for ecological niches with other bacteria. Compared to eukaryotic AMPs, bacteriocins are more potent and have a narrower spectrum effective against more closely related species (Hassan et al., 2012).

In terms of structure, most AMPs are short (possessing 10-50 amino acids), have a global positive charge, and are amphipathic with a significant proportion of hydrophobic residues. Their cationic nature is due to an abundance of positively charged amino acids (arginine, lysine, and histidine). Their secondary structure usually falls into three types: alpha-helical, beta-sheet and random-coil. Alpha-helical peptides are unstructured in aqueous solution but adopt an amphipathic configuration when in contact with biological membranes; beta-sheet peptides are stabilized by disulfide bonds and are more rigid; random-coil AMPs are less frequent and lack a defined structure, but also undergo a transformation when approaching membranes (Mahlapuu et al., 2016).

3.2. Mechanism and selectivity

The main established mechanism of AMPs is the disruption of the physical integrity of microbial membranes, which is thought to explain their broad-spectrum activity. Regarding bacteria, there is an initial electrostatic attraction between the cationic AMPs and the negatively charged membrane, which then promotes insertion in the phospholipid bilayer. The negative membrane charge of bacteria is a result of phospholipids with negatively charged head groups – namely phosphatidylglycerol, cardiolipin and phosphatidylserine. Other molecules with negative charge further promote interaction

with AMPs: teichoic acids (TAs) in the cell wall of Gram-positive bacteria, and lipopolysaccharide (LPS) in the outer membrane of Gram-negative bacteria.

In contrast, mammalian cell membranes are richer in zwitterionic phospholipids such as phosphatidylethanolamine, phosphatidylcholine, and sphingomyelin – which results in a neutral net charge. Besides, zwitterionic phospholipids are more abundant in the outer leaflet, while anionic phospholipids are confined to the inner leaflet. This difference in charge, together with a less negative transmembrane potential, contributes to interaction with AMPs being of hydrophobic nature, weaker than electrostatic interactions. Cholesterol may also have a protective effect through membrane stabilization (Mahlapuu et al., 2016). Overall, these differences help explain the observed selectivity of AMPs to bacterial cells. Because, like bacteria, tumor cell membranes are rich in the negative lipid phosphatidylserine, AMPs also show potential as anticancer agents (Deslouches & Peter Di, 2017).

There are three main models that explain AMP interaction with membranes (figure 3): the barrel-stave model states that peptides are inserted perpendicularly in the membrane and form a pore by association with each other; the toroidal-pore model states that peptides insert perpendicularly but induce membrane conformations that lead to a pore lined by peptides and phospholipid head groups; and the carpet model states that peptides adsorb parallelly to the cell surface and their accumulation causes disintegration and formation of micelles (Andersson et al., 2016). Despite these established mechanisms, molecular dynamics simulations have shown that some peptides can permeate lipid bilayers without pore formation (Ulmschneider, 2017).

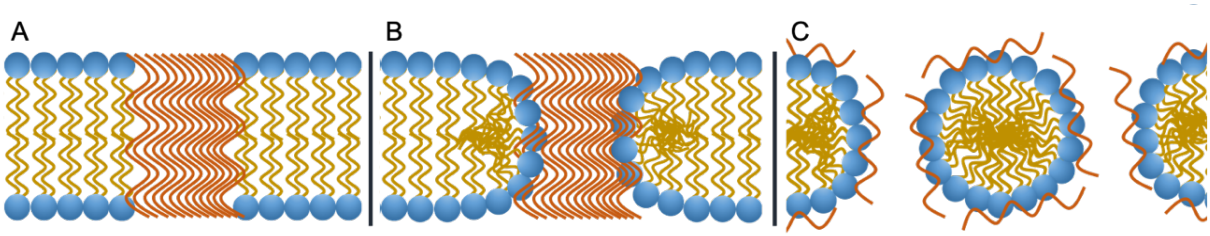

Figure 3 - Main mechanisms of AMP interaction with bacterial membranes: the barrel-stave model (A), the toroidal-pore model (B) and the carpet model (C).

Different mechanisms have been described for the same AMP, with some having membrane-disrupting activity as well as other cellular targets. Some AMPs affect protein biosynthesis and metabolism, cell division, and intracellularly bind ribosomes, chaperone proteins, proteases, DNA and RNA, and external structures such as capsule polysaccharides, cell wall peptidoglycan, and outer membrane components. For example, indolicidin is an AMP of bovine origin which binds both DNA and enzymes involved in DNA metabolism (Cheng-Foh & Chee-Mun, 2017).

Besides direct microbicidal activity, AMPs can also have immunomodulatory activity that indirectly contributes to resolution of infection. High AMP concentrations have been shown to lead to chemoattraction of inflammatory cells as well as to regulation of inflammatory activity. Although produced as part of innate immunity, AMPs can also act as a bridge to adaptive immunity by attracting antigen-presenting cells (APCs) and modulate the adaptive response by promoting lymphocyte differentiation. Interestingly, there also appears to be an interaction between AMP expression and the composition of skin and gut microbiota, which in turn influences activity against invading pathogens. The human cathelicidin LL-37 is likely the AMP with best studied immune function, with studies reporting chemotaxis of neutrophils, eosinophils, monocytes, T cells and mast cells; inhibition of neutrophil apoptosis; macrophage polarization into an M1 phenotype; LPS neutralization; induction

of expression of anti-inflammatory cytokines, among others (van der Does et al., 2019). Immunomodulatory activity has also been characterized in synthetic AMPs developed from natural peptides, through modulation of macrophage phenotype, cytokine expression, and leukocyte recruitment (Barrero-Guevara et al., 2019; Silva et al., 2016).

Finally, both natural and synthetic AMPs have been shown to influence essential processes of skin wound healing (figure 4). These include receptor signaling mechanisms responsible for cell proliferation and migration, such as the epidermal growth factor receptor (EGFR); re-epithelialization and granulation tissue formation; angiogenesis through induction of endothelial cell tube formation and upregulation of angiogenic proteins and VEGF; and also fibroblast differentiation and collagen production (Thapa, Diep, et al., 2020).

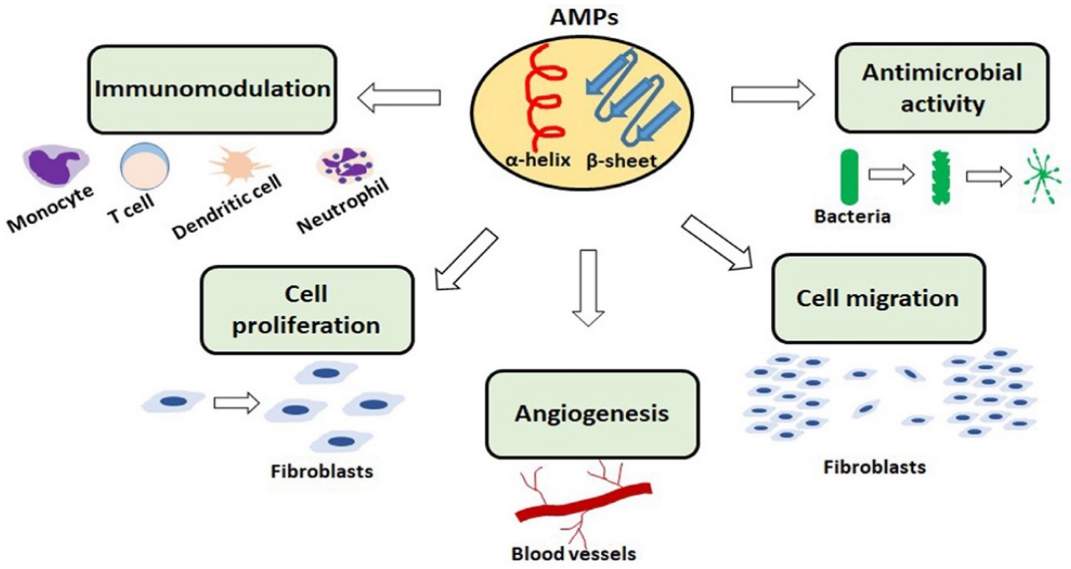

Figure 4 - Reported mechanisms of AMPs in the context of wound healing (Thapa, Diep, et al., 2020).

3.3. Resistance

Because of their nonspecific multiple-target mechanism, membrane interference and fast action, AMPs have a smaller risk of inducing development of resistance in bacteria when compared to conventional antibiotics (which normally have a single enzymatic target). This is because drastic alterations in cell membrane composition could lead to loss of functional and structural integrity in bacteria (Thapa, Diep, et al., 2020). Even so, cases of bacterial resistance to AMPs have been described in the literature.

(Andersson et al., 2016) provides a thorough overview of the identified mechanisms of bacterial resistance to AMPs. As bacteria have evolved in the presence of AMPs from both bacterial and eukaryotic origin, resistance has inevitably appeared. For instance, passive resistance can occur by incorporation of positively charged molecules in the membrane. The addition of 4-aminoarabinose (Ara4N) to lipid A, a component of LPS, leads to a less negative charge of the outer membrane of Gram-negative bacteria (Manniello et al., 1978; Viljanen & Vaara, 1984). *P. aeruginosa* and other species can also neutralize AMPs by binding to anionic capsular polysaccharides (Llobet et al., 2008). For Gram-positive bacteria, these alterations take place in the TAs of the cell wall. In *S. aureus*,

resistance can be conferred by D-alanylation of TAs, incorporation of lysylphosphatidylglycerol in the cell membrane, activation of the AMP transporter vraFG, and addition of L-lysine to membrane phospholipids (Ernst et al., 2009; M. Li et al., 2007). Other intrinsic methods of resistance are removal by efflux systems (such as the ABC transporter-dependent efflux pump in *S. aureus*) and degradation by proteases.

On the other hand, acquired resistance consists of microorganisms becoming resistant to an agent to which they were previously susceptible. An example of this would be the naturally-occurring small colony variant (SCV) phenotype described for *S. aureus* – with slow growth rate and altered transmembrane potential – resistant to LL-37 and other AMPs (Gläser et al., 2014; Samuelsen et al., 2005b). *S. aureus* resistance has also been experimentally induced for lactoferricin B (Samuelsen et al., 2005a) and pexiganan (Habets & Brockhurst, 2012). In some cases, AMP exposure caused development of cross-resistance to other AMPs and was maintained after passage to AMP-free medium. Unlike with antibiotics, the mutation rate and fitness of the resulting mutants after AMP exposure have been poorly investigated, but existing results suggest they are comparable to those caused by standard antibiotics.

Resistance at the clinical level has not been well assessed due to the lack of AMPs approved for clinical use. VRSA is the most prominent example of an AMP-resistant strain, though its mechanism does not involve membrane disruption – which, as mentioned above, makes resistance less likely. However, there is a concern that widespread use of AMPs could lead to development of cross-resistance to peptides that are part of the human immune system. Thus, the phenomenon of AMP resistance will have to be monitored before their general application.

3.4. History and development

Based on PubMed data, research into peptide drugs as antimicrobial agents started halfway through the 20th century, similarly to antibiotics in general. The number of papers published per year grew steadily at first and was followed by an upsurge in the 1980s, which overlaps with the abovementioned growing awareness of antibiotic resistance (figure 5). Despite AMP investigation sometimes being viewed as a recent development, some have been on the market for more than 50 years. A summary of the antibacterial AMPs approved by FDA is presented in table 1.

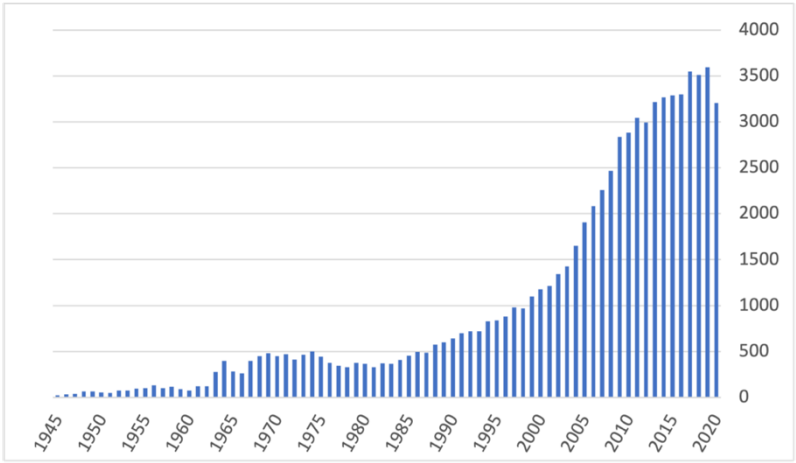

Figure 5 - Evolution of the number of published papers per year using the search words "antimicrobial peptide" in PubMed.

While most of these polypeptide antibiotics have membrane-disrupting activity, the main antimicrobial mechanism of bacitracin and vancomycin is the inhibition of cell wall peptidoglycan synthesis. Effectively, all these AMPs were isolated from soil bacteria and can therefore be classified as bacteriocins. In terms of structure, some have cyclic structures and lipid components which might contribute to their stability (Chen & Lu, 2020). Most of these molecules are only effective against Gram-positive organisms, which could be explained by the outer membrane of Gram-negative bacteria posing as a barrier to reaching the cell membrane. This presents a clear disadvantage for treating polymicrobial infections and denotes a lack of antibiotics effective against Gram-negative bacteria.

Table 1 - List of currently FDA-approved antibacterial AMPs (Antimicrobial peptides - Wikipedia, n.d.; Koo & Seo, 2019).

Name	Year of approval	Main mechanism	Indication	Administration	Reference
Bacitracin	1948	Inhibition of cell wall peptidoglycan synthesis	Treatment and prevention of Gram-positive skin and eye infections	Topical, ophthalmic, intramuscular	(Toscano & Storm, 1982)
Gramicidin D	1955	Cell membrane disruption	Treatment of bacterial conjunctivitis	Topical, ophthalmic	(Hallett et al., 1956)
Colistin (Polymyxin E)	1962	Cell membrane disruption	Last-resort treatments of multidrug-resistant Gram-negative infections	Inhalation, intramuscular, intravenous	(Kwa et al., 2007)
Polymyxin B	1964	Cell membrane disruption		Intravenous, intramuscular, intrathecal, ophthalmic	
Vancomycin (and derivatives **oritavancin, dalbavancin** and **telavancin)**	1983	Inhibition of cell wall peptidoglycan synthesis	Treatment of complicated MRSA infections	Intravenous	(Hermans & Wilhelm, 1987)
Daptomycin	2003	Cell membrane disruption	Treatment of complicated skin infections	Intravenous	(Carpenter & Chambers, 2004)

Interest in AMPs resurfaced recently due to the growing threat of AMR, with a focus on developing broad-spectrum agents with reduced probability of resistance. Numerous peptides are in preclinical and clinical development as antimicrobials, of which pexiganan (or MSI-78) is probably the best studied (Gottler & Ramamoorthy, 2009). It is a 22-amino-acid peptide derived from magainin-2, a natural AMP discovered in 1987 in the skin of the African frog *Xenopus laevis* (Zasloff, 1987). Pexiganan has a random coil structure in solution and forms an alpha-helix dimer in the presence of lipids. It was found to have broad-spectrum antibacterial and antifungal activity due to membrane disruption through a toroidal pore mechanism (Ge et al., 1999). In 1994, pexiganan acetate cream was put to the test in two consecutive clinical trials for treating diabetic foot ulcer (DFU) infections, where it proved equally effective to the oral antibiotic ofloxacin (Lipsky et al., 2008). More recently, though, it failed to prove superior to a placebo in two parallel phase 2 trials (registration numbers NCT01590758 and NCT01594762).

Other notable examples of antibacterial AMPs in development are the human cathelicidin LL-37, with a phase 2 clinical trial for treatment of DFUs already in motion (registration number NCT04098562) and a completed phase 2 trial on venous leg ulcers (Grönberg et al., 2014); murepavadin (or POL7080), a protegrin analog which was the focus of a phase 2 trial on *P. aeruginosa* pneumonia (registration number NCT02096328); and lytixar (or LTX-109), a synthetic peptide successfully tested in patients with nasal colonization by methicillin-sensitive *S. aureus* (MSSA) and MRSA (Nilsson et al., 2015).

As of September 15th 2021, there are 22 259 entries in the DRAMP database (Data Repository for Antimicrobial Peptides), of which 77 are currently in drug development (Kang et al., 2019). DBAASP (Database of Antimicrobial Activity and Structure of Peptides) provides more details regarding AMP origin, with 82.6 % being synthetic, and 80 % of natural AMPs originating in the animal kingdom. Furthermore, the majority of peptides target bacteria, with a slight advantage for Gram-negative organisms (Pirtskhalava et al., 2021).

3.5. Strategies to improve AMP effectiveness

Despite the good efficacy, safety and tolerability, predictable metabolism, high selectivity, and potency of peptide drugs in general, they are usually chemically unstable, prone to hydrolysis or oxidation and aggregation, have a short half-life, low oral bioavailability and high production costs when compared to small molecule drugs (Fosgerau & Hoffmann, 2015). These factors contribute to the often-observed discrepancies between in vitro and in vivo efficacy of AMPs. On the other hand, components of the mammalian physiological environment may boost AMP activity, which is not replicated in the usual in vitro assays. Due to this, a great portion of AMPs developed to date have been directed for local application in the form of creams or sprays (Thapa, Diep, et al., 2020).

3.5.1. Delivery route

The low oral bioavailability of AMPs stems from enzymatic degradation and poor penetration of the intestinal mucosa. In the case of intravenous administration, AMPs can cause toxicity to red blood cells (hemolysis) and other cell types by membrane destabilization. Besides, opsonization or binding to serum proteins leads to fast clearance by the reticuloendothelial system and prevents them from reaching their therapeutic target.

In this regard, combination with polyethylene glycol (PEG) – with or without nanoparticles (NPs) – is commonly performed, in a process termed "PEGylation". PEG is a hydrophilic, non-ionic, inert polymer that reduces aggregation, opsonization and phagocytosis, for which it is often classified as a "stealth polymer". As a result, it can increase circulation time (in case of systemic administration) or residence time (for local applications such as in wounds) of drugs (Suk et al., 2017).

Dermal AMP delivery in wounds has the benefits of evading hepatic first-pass metabolism, increasing bioavailability, reducing dosing frequency, non-invasiveness, and accessibility. These contribute to patient compliance and limit development of resistance (Manikkath et al., 2018). However, aggregation and degradation by wound proteases can still limit local AMP effectiveness.

3.5.2. Structural modifications

Peptide structure can also be tweaked to increase AMP stability and efficacy. Common strategies include cyclization, incorporation of non-natural or D-enantiomeric amino acids, use of peptide mimetic structures, and terminal functionalization by acetylation or other methods (Mahlapuu et al., 2016). Furthermore, attempts have been made to improve the properties of existing AMPs by amino acid substitution or sequence truncation or selection (Park et al., 2007; Subbalakshmi et al., 1999).

3.5.3. Nanoparticles (NPs) as drug carriers

Another prominent strategy to improve AMP effectiveness is using NPs as carriers to the site of infection. Nanotechnology, being the engineering of materials with dimensions typically between 1 and 100 nm, is today an emerging field of science due to the distinctive physicochemical and biological properties of entities at this scale. In the health sector, nanomedicine has erupted with diverse applications in diagnostics and delivery of therapeutic agents. NPs in general are valuable as they can increase oral bioavailability and cellular uptake of drugs, allow a targeted delivery and controlled release, and increase tissue penetration. NPs can be engineered to accommodate the various physicochemical properties of drugs, and their size, shape, wettability, and surface properties can be altered to modulate their behavior. Because of this, the inclusion of pharmaceutical compounds in NPs can potentially improve their solubility, release profile, diffusivity and immunogenicity (Patra et al., 2018).

NPs have been proposed and studied as treatments for infection, since they can overcome bacterial resistance mechanisms (by increasing uptake and decreasing efflux of their contents), penetrate or destroy biofilms, and reach intracellular bacteria. When using oral or intravenous routes, targeting of antimicrobial agents to the site of infection can be done via a passive method – the enhanced permeation and retention (EPR) effect caused by inflammation – or an active method (specific ligand binding), which can increase concentration in the place of interest and therefore reduce the necessary dose, probability of resistance, and effects on the host (Pelgrift & Friedman, 2013). NPs can also be engineered to be environmentally responsive to cues present in infected tissues, such as altered temperature, pH, redox potential and enzymatic activity, or to react to external stimuli like electric and magnetic fields (W. Gao et al., 2014).

Besides improving AMP effectiveness, some types of NPs also have intrinsic antimicrobial and wound healing properties. Certain types are associated with improved inflammation and proliferation phases, and a select few aid in hemostasis and remodeling (Kalashnikova et al., 2015). Direct antimicrobial activity is mostly reported for metallic NPs through the release of metal ions and

oxidative stress. Other non-oxidative mechanisms include disruption and penetration of bacterial cell membranes, and intracellular interaction with proteins and DNA (Wang et al., 2017).

3.5.3.1. Types of conjugation

Drug loading is the most common conjugation technique for drugs in general and for AMPs. By allowing a gradual release, the therapeutic effect is prolonged and the drug is protected from proteolytic and environmental degradation while inside the NPs. The volume and lack of organization inside the NPs can grant higher AMP concentrations but does not prevent aggregation. Surface immobilization, on the other hand, can prevent AMP aggregation and allows a homogeneous surface distribution. Furthermore, as the peptide is tethered to the outer NP surface, the antimicrobial activity is faster and its effectiveness is not dependent on the release rate. This strategy also allows to maintain AMP targeting and selectivity to bacterial cells, which contributes to efficacy and potentially reduces toxicity to host cells.

A list of the various types of NPs that have been used as carriers for AMPs can be found in table 2. While the obvious choice for smaller NPs like gold (AuNPs), silver (AgNPs) and quantum dots (QDs) is surface immobilization of AMPs, loading is the most common strategy for polymeric and lipid NPs. The high surface area of mesoporous silica nanoparticles (MSNs) allows to obtain high AMP functionalization with adsorption alone. Even so, there are some examples of AMPs being functionalized in polymeric NPs and adsorbed to lipid nanocapsules (Umerska et al., 2017a; Vijayan et al., 2019), which leaves open the possibility of loading other molecules relevant to wound healing. It is noticeable that the combination of AMPs with metallic NPs has been by far further explored than with other types of NPs, which is likely due to their established antibacterial activity.

Table 2 - A summary of the different types of NPs that have been conjugated with AMPs. AMPs are represented as orange in the figures (not drawn to scale).

Material	Type of nanoparticles (NPs)	Type of conjugation	Representation	References
Polymeric	Chitosan	Loading	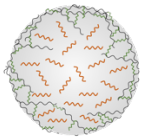	(Almaaytah et al., 2017; Piras et al., 2015; Sun et al., 2018)
	Poly(lactic-co-glycolic acid) (PLGA) / Polylactic acid (PLA)	Loading	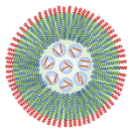	(Chereddy et al., 2014; Cruz et al., 2017)
		Covalent immobilization	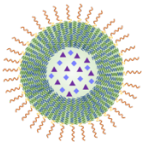	(Vijayan et al., 2019)
	Dendrimers	Covalent immobilization	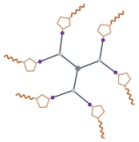	(Fernandez et al., 2019; Pires et al., 2015)

Lipid	Solid lipid nanoparticles (SLNs)	Loading	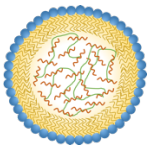	(Severino et al., 2017)
	Nanostructured Lipid Carriers (NLCs)	Loading	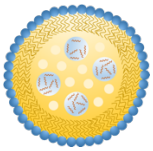	(Garcia-orue et al., 2016)
	Lipid nanocapsules	Loading	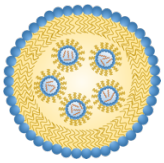	(Groo et al., 2018)
		Surface adsorption	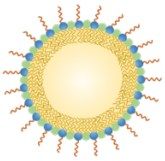	(Umerska et al., 2017b)
	Cubosomes	Loading / surface adsorption	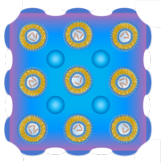	(L. Boge et al., 2017, 2018; Meikle et al., 2017)
Metallic	Gold (AuNPs)	Covalent immobilization	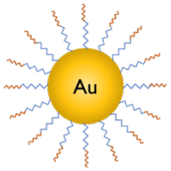	(Casciaro et al., 2017; W. Y. Chen et al., 2015; Jalaei et al., 2018; Wadhwani et al., 2017)
	Silver (AgNPs)	Covalent immobilization	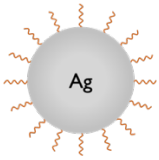	(J. Gao et al., 2019; Lambadi et al., 2015; McLaughlin et al., 2016; Pal et al., 2019)
	Magnetic (MNPs)	Covalent immobilization / adsorption	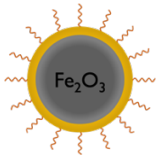	(Maleki et al., 2016; Piktel et al., 2019)
Semiconductor	Quantum dots (QDs)	Covalent immobilization / adsorption	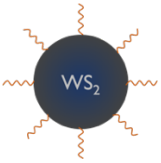	(Abdul et al., 2019; Galdiero et al., 2016; Mazumdar et al., 2020)
Ceramic	Mesoporous silica nanoparticles (MSNs)	Surface adsorption	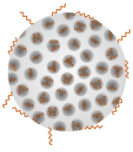	(Braun et al., 2016, 2017; Gounani et al., 2018)

Altogether, NPs show great promise to improve the effectiveness of established potent AMPs and avoid the loss of activity often seen when translating to the in vivo setting. In this way, nanotechnology might play a role in helping more of these molecules reach the clinical stage as a more effective and sustainable alternative to conventional antibiotics in treating chronic bacterial infections.

4. Poly(lactic-co-glycolic acid)

Among the materials listed above, PLGA possesses properties that make it interesting for wound healing applications. In general, biodegradable synthetic polymers retain the main advantage of natural polymers while having fewer concerns regarding purity and stability (Cruz et al., 2017). PLGA is a non-toxic, biodegradable, hydrophobic synthetic polymer widely used in drug delivery. It has been used as material for absorbable sutures (Gilding & Reed, 1979) and is also FDA-approved in the form of microsphere injections for the treatment of cancer, diabetes and other diseases since 1989 (Zhong et al., 2018).

PLGA degrades into lactic acid (LA) and glycolic acid (GA) when in contact with water, endogenous molecules that can be metabolized via the Krebs cycle (Danhier et al., 2012; Mir et al., 2017). Initial degradation causes an autocatalytic effect in which the increased acidity accelerates further degradation. The polymer's degradation rate is mainly dependent on the initial molecular weight (M_w), monomer composition (LA:GA ratio), the type of drug conjugated, processing method, and pH of the release medium. A lower M_w of PLGA leads to NPs having reduced hydrophobicity, which accelerates water absorption, hydrolysis, and erosion. Because LA contains an additional methyl side chain, it is more hydrophobic and has a slower degradation rate than GA. Therefore, higher contents of GA lead to faster PLGA degradation. Adjusting these parameters allows to tune the degradation rate and control drug release for specific applications (Mir et al., 2017).

However, the main property of PLGA that justifies its potential in wound healing is the release of lactate, naturally produced in wounds during the initial hypoxic phase (Chereddy et al., 2016). This molecule is known to serve as signal for collagen synthesis, angiogenesis, and wound repair. These effects have been confirmed in vivo using subcutaneous PLGA implants (Porporato et al., 2012) and PLGA NPs (Chereddy et al., 2014). Because the inclusion of GA accelerates polymer degradation, PLGA has been found to promote a more sustained LA release compared to polylactic acid (PLA). One disadvantage of hydrophobic NPs such as PLGA is surface adsorption by proteins, which can prevent them from reaching their target and triggering a therapeutic effect. To address that, functionalization with PEG is often employed, as explained above.

5. MSI-78(4-20)

MSI-78(4-20) is a 17-residue peptide designed by our group developed by spanning part of the sequence of pexiganan or MSI-78 (table 3), which is the best studied AMP to date (Monteiro et al., 2015). This cost-effective AMP was similarly effective to the parent peptide against tested trains of *S. aureus*, MRSA, *S. epidermidis* and *P. aeruginosa*, and was the most effective out of six designed

peptides. It showed considerably reduced hemolytic activity against human red blood cells when compared to pexiganan (figure 6A).

Also, interaction studies were made with membrane models of eukaryotic and bacterial cells, composed of 1,2-dimyristoyl-sn-glycero-phosphocholine (DMPC) and equal parts of 1-palmitoyl-2-oleoyl-sn-glycero-3-phosphocholine (POPC) and 1-palmitoyl-2-oleoyl-sn-glycero-3-phosphoglycerol (POPG), respectively. While there was no significant difference in the zeta potential (ZP) and hydrodynamic diameter of DMPC vesicles after AMP addition, there was a concentration-dependent increase in both parameters for POPC:POPG models, as well as high polydispersity. This suggests the interaction of MSI-78 and MSI-78(4-20) is more selective to bacterial membranes, in which AMP interaction and aggregation take place.

In terms of AMP properties, MSI-78(4-20) has a slightly lower net charge (+7) than MSI-78 (+9), a lower percentage of helicity (33 % compared to 62 % for MSI-78), and a higher hydrophobicity. The authors propose that while MSI-78 might have more intense electrostatic interactions with bacterial membranes due to its higher charge, the higher hydrophobicity of MSI-78(4-20) may allow a deeper insertion into the bilayers, which explains its similar efficacy.

More recently, MSI-78(4-20) was covalently immobilized in chitosan coatings and tested against *Staphylococcus epidermidis* (Monteiro et al., 2020). Immobilization was achieved through a succinimidyl-[(N-maleimidopropionamido)-octaethyleneglycol] ester ($SM(PEG)_8$) crosslinker. Antimicrobial activity was assessed through bacterial adhesion and viability in phosphate-buffered saline (PBS) and PBS supplemented with 1 % human plasma. While bacterial adhesion did not significantly vary between samples, high and similar percentages of death were obtained for surfaces with AMP immobilized by either terminal, in PBS. In the presence of human plasma, there was a significant decrease in bacterial adhesion with AMP compared to chitosan controls exposed to reaction buffer, and AMP surfaces caused 76 % of death when bound by either terminal, higher than in PBS (figure 6B). These results suggest covalent immobilization of MSI-78(4-20) is promising in terms of antimicrobial efficacy in the complex in vivo environment.

Table 3 - Sequences and length of pexiganan (MSI-78) and its derivative MSI-78(4-20). Adapted from (Monteiro et al., 2015).

peptides	amino acid sequence
MSI-78	GIGKFLKKAKKFGKAFVKILKK 22 AA
MSI-78(4–20)	—KFLKKAKKFGKAFVKIL— 17 AA

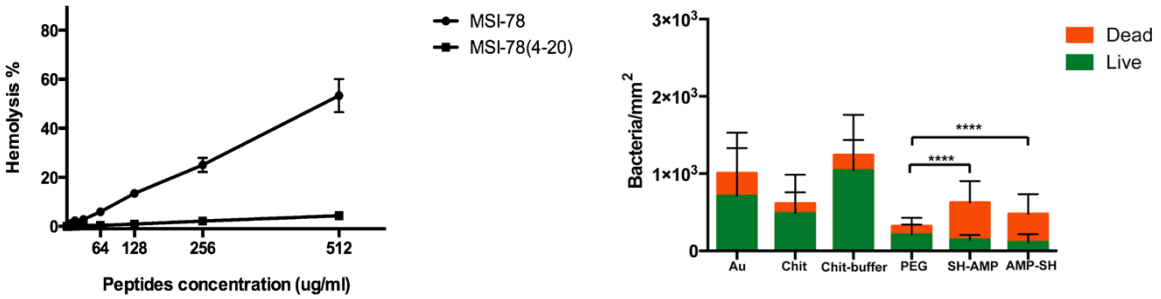

Figure 6 - (A) Percentage of hemolysis at different concentrations of MSI-78 and MSI-78(4-20), showing the reduced hemolytic activity of MSI-78(4-20) (Monteiro et al., 2015). (B) Quantification of bacterial adhesion and viability to chitosan films with immobilized MSI-78(4-20) in medium supplemented with human plasma. Gold substrate (Au); unmodified chitosan films (Chit) and chitosan exposed to reaction buffer (Chit-buffer); chitosan films modified with succinimidyl-[(N-maleimidopropionamido)-octaethyleneglycol] ester ($SM(PEG)_8$) (PEG); and chitosan films modified with AMP (SH-AMP/AMP-SH) (Monteiro et al., 2020).

Aim

AMPs have the potential to become the next anti-infective agents in a world where chronic wounds are becoming more prevalent and antibiotic resistance is inevitably spreading. Nanotechnology can be used to improve on AMP properties, bridging the gap between the Petri dish and the complex in vivo environment. In this work, we combine these two emerging technologies to create a novel strategy to fight wound infections.

In this approach, polymeric NPs – composed of poly(lactide-co-glycolide acid)-polyethylene glycol (PLGA-PEG) and PLGA-PEG-maleimide (PLGA-PEG-Mal) copolymers – were produced by nanoprecipitation and later surface-functionalized with the cysteine-modified AMP MSI-78(4-20)-Ahx-Cys developed by our group (Monteiro et al., 2015). Maleimide (Mal) was used to provide covalent binding between AMP and NPs, as it binds to the thiol groups of cysteine (Kim et al., 2008). For that purpose, a cysteine (Cys) residue was added to the C-terminal of MSI-78(4-20) via a 6-aminohexanoic acid (Ahx) linker. This approach allows stable and site-specific interactions as well as a homogeneous surface distribution of the AMP. Surface immobilization was used instead of loading because it allows to benefit from the general advantages of combination with NPs (protection from protease degradation and aggregation, mainly) while maintaining immediate action and treatment selectivity to bacteria due to AMP electrostatic interactions. The non-fouling nature of PEG can also increase AMP exposure by preventing folding and adsorption to NPs. These features may lead to an increase in effectiveness which, in turn, decreases toxicity to mammalian cells by requiring smaller doses of AMP.

Specifically, the first goal of this work was to combine the AMP with NPs and characterize the resulting conjugate in terms of size distribution, charge, morphology, and AMP immobilization efficiency. Secondly, to test the antimicrobial activity of the AMP-NPs against relevant bacterial strains in normal growth medium and in a simulated wound fluid that mimics the in vivo wound environment, to determine the effective AMP concentrations. In addition, killing kinetics and antibiofilm activity against a biofilm-forming strain were studied.

As a whole, this work aims to contribute to the successful implementation of AMPs in the clinical setting and to find solutions for the antimicrobial resistance crisis, while taking advantage of the role of nanotechnology and NPs in drug delivery.

Materials and methods

1. AMP-NP production

1.1. NP production

NPs were produced by nanoprecipitation through a solvent displacement method. Polyethylene glycol-poly(lactide-co-glycolide) (PLGA-PEG) and poly(D,L-lactide-co-glycolide)-polyethylene glycol-maleimide (PLGA-PEG-Mal) solid copolymers (50:50 LA:GA) (PolySciTech; Indiana, USA) were mixed to obtain NPs with different amounts of maleimide in a final mass of 20 mg. Three PLGA-PEG : PLGA-PEG-Mal mass ratios were made – 9:1 (10%Mal), 8:2 (20%Mal) and 6:4 (40%Mal). The properties of the polymers used in NP production can be seen in table 4. After weighing the polymers, 1 mL of acetone (Sigma, Missouri, USA) was added and the samples were vortexed until complete dissolution. The following steps were done in sterile conditions. NPs were formed by slowly dispensing the polymer solutions in 10 mL of type I ultrapure water (Milli-Q, Merck, Darmstadt, Germany) while agitating at 230 rpm for 2 hours.

Meanwhile, centrifugal filter units with 100 kDa nominal molecular weight limit (NMWL) (Amicon, Merck) were sterilized by centrifuging once with 10 mL of ethanol 70 % (v/v) for 10 minutes at 2500 rpm and twice with 10 mL of ultrapure water in a 5810R centrifuge (Eppendorf, Hamburg, Germany). The NP suspensions were then transferred to the filters and centrifuged for 10 minutes at 2500 rpm. The same procedure was done to wash NPs with ultrapure water twice and once in phosphate buffer (pH 6.6), composed of 0.0625 M sodium phosphate dibasic dihydrate ($NaH_2PO_4 \cdot 2H_2O$) and 0.0375 M sodium phosphate monobasic dihydrate (Na_2HPO_4) (Sigma) in type II ultrapure water. In this last step, NP suspensions were collected in a volume of 800 µL of phosphate buffer.

1.2. AMP immobilization

Cysteine-modified MSI-78(4-20) (MSI-78(4-20)-Ahx-Cys) (table 4) was produced by solid-phase peptide synthesis (SPPS) at Paula Gomes Lab (REQUIMTE, Departamento de Química e Bioquímica (DQB), Faculdade de Ciências da Universidade do Porto (FCUP), Portugal). Surface immobilization was achieved by a maleimide-thiol Michael Addition reaction (figure 7). For that, 200 µL of AMP dissolved in phosphate buffer (pH 6.6) were added to the 800 µL of NP suspension to achieve 1:2.5 Mal-AMP molar ratio. Control samples were adjusted to 1 mL with phosphate buffer. Samples were left to agitate at 110 rpm overnight in an orbital shaker (Panasonic, Osaka, Japan). On the following day, all samples were transferred to sterilized Amicon filter units and washed three times with 10 mL of

ultrapure water. In the last wash, samples were centrifuged until residual volumes were below 1 mL (standard procedure) or 500 µL (to obtain higher AMP-NP concentrations). The washing steps in this protocol allow to remove free polymer and unbound AMP. The samples were stored at 4 °C. A representation of the NPs produced using this protocol can be found in figure 8.

Table 4 - Chemical properties of the polymers and peptide used in AMP-NP production.

Component	Sequence	Molecular Weight (Da)
PLGA-PEG	Methoxy-$(PEG)_n$-$(LA\text{-}GA)_n$	3 000 - 36 000
PLGA-PEG-Mal	Mal-(N-(2-aminoethyl)-methoxyamide)-$(PEG)_n$-$(LA\text{-}GA)_n$	30 000 - 5 000
MSI-78(4-20)	KFLKKAKKFGKAFVKIL-Ahx-Cys	2 211

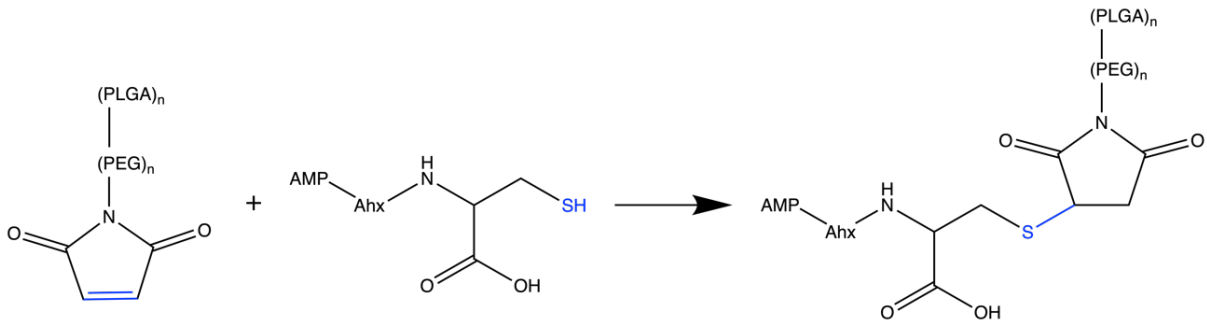

Figure 7 - Representation of the thiol-maleimide reaction between PLGA-PEG-Mal and cysteine-modified MSI-78(4-20) (MSI-78(4-20)-Ahx-Cys).

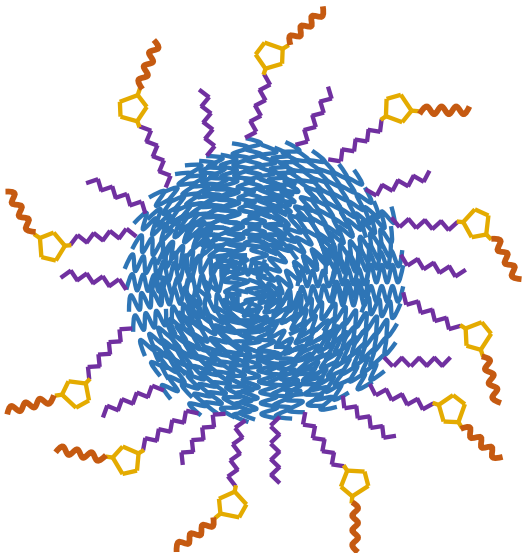

Figure 8 - Scheme of the NPs used in this project: NPs are composed of a mixture of PLGA-PEG and PLGA-PEG-Mal copolymers with AMPs covalently immobilized via maleimide-thiol chemistry. PLGA is represented as blue, PEG as purple, Mal as yellow, and MSI-78(4-20)-Ahx-Cys as orange.

2. AMP-NP characterization

2.1. Dynamic light scattering (DLS) and laser Doppler anemometry

Size, polydispersity index (PdI) and zeta potential (ZP) measurements were made in a Zetasizer Nano ZS equipment (Malvern Instruments, Malvern, UK) at the Biointerfaces and Nanotechnology scientific platform of Instituto de Investigação e Inovação em Saúde (i3S), Universidade do Porto, Portugal. The size analysis is based on dynamic light scattering (DLS), in which the particle solution is placed in the path of a monochromatic beam of light and an opposing detector measures the intensity of scattered light throughout time due to the particles' Brownian motion, which is correlated with hydrodynamic diameter. Surface charge is measured by laser Doppler anemometry, which is similar to DLS but instead an oscillating electric field is responsible for particle motion between two electrodes.

Samples were diluted 1:100 in sodium chloride (NaCl) 10 mM (Honeywell, North Carolina, USA). An electrode-containing folded capillary cell (DTS1070) (Malvern Instruments) was used for measuring all samples and was washed with ultrapure water between measurements. Size measurements were done at 25.0 ºC after an initial equilibration time of 60 seconds, at a measurement angle of 173 º (backscatter), with 3 measurements of 11 runs each, according to the Smoluchowski model. Zeta potential was measured with 3 measurements of 10-100 runs with a 15 second delay and automatic voltage selection. Zeta potential was measured after particle size, as it may damage the samples.

2.2. Nanoparticle tracking analysis (NTA)

NP concentrations were determined by nanoparticle tracking analysis (NTA) in a NanoSight NS300 NTA Dev Build 3.2.16 equipped with an sCMOS camera (Malvern Instruments). For this analysis, sequential dilutions with ultrapure water of 1:40, 1:500 and 1:10 were prepared from the samples to obtain a concentration within a scale of magnitude of 10^8 NP/mL. In brief, three movies of 30 seconds were recorded for each sample (with a threshold of 10 to 50 particles per frame), with the following capturing settings: camera level 15, slider shutter 1206, slider gain 366, at 23 ºC, and with a syringe pump speed of 40. Data acquisition and processing were performed using the NanoSight NS300 NTA 3.0 software, using a detection threshold of 5. Analysis was performed by Cecília Durães and Ana Rita Pinto at i3S. This technology measures scattered light similarly to DLS, but records particle movement with a camera and analyzes hydrodynamic diameter on an individual basis. Therefore, besides providing NP quantification, it also allows a more detailed study of particle size.

2.3. Transmission electron microscopy (TEM)

Transmission electron microscopy (TEM) was used to assess the morphology of the NPs. The suspensions were diluted 1:10 in ultrapure water. A copper-mesh grid was used to place 10 µL of NP

suspension for 2 minutes. The excess of NPs was then removed and 10 µL of 1 % (w/v) uranyl acetate solution was added to the grid for 5 seconds at room temperature (negative staining). The samples were observed in a JEM-1400 Transmission Electron Microscope (JEOL Ltd., Tokyo, Japan) with an acceleration voltage of 80 kV. Analysis was performed at the i3S Histology and Electron Microscopy scientific platform.

2.4. Fourier-transform infrared (FTIR) spectroscopy

Fourier-transform infrared (FTIR) spectroscopy was used to characterize the NPs and detect AMP on the samples. Samples were dried for 1 hour at room temperature on a vacuum oven (Binder, Tuttlinger, Germany). 5 mg of each sample were mixed with 200 mg of potassium bromide (KBr) powder (Specac, Orpington, UK) and compressed into a pellet that was loaded into a Frontier 2000 FT-IR spectrometer (PerkinElmer, Massachusetts, USA) with a mid-infrared (MIR) triglycine sulfate (TGS) detector at the i3S Biointerfaces and Nanotechnology scientific platform. The spectra were obtained using 32 scans, at a spectral resolution of 4 cm^{-1}, and wavenumber ranging from 4000 to 400 cm^{-1}.

2.5. Nuclear magnetic resonance (NMR) spectroscopy

Covalent binding between Mal and AMP was assessed by proton nuclear magnetic resonance (^{1}H-NMR) spectroscopy. NMR spectra were acquired with an Avance III 400 MHz spectrometer (Bruker, Massachusetts, USA) in $CDCl_3$ and processed using MestReNova software. Chemical shifts are reported in ppm (δ units) and were referenced to the residual solvent signals. Analysis was performed at Centro de Materiais da Universidade do Porto (CEMUP) by Victoria Leiro from i3S.

2.6. Fluorescamine assay (AMP quantification)

AMP quantification in each sample was achieved by fluorometric analysis with fluorescamine based on the protocol developed by (Held, 2006). Fluorescamine reacts with the primary amino groups of terminal amino acids and lysine, originating a fluorescent pyrrolinone moiety. Firstly, a calibration curve correlating peptide concentration with fluorescence intensity was obtained using known concentrations of AMP. For that, the peptide was dissolved in ultrapure water to obtain a 1024 µg/mL solution and 150 µL were added to 150 µL of ultrapure water in a black 96-well plate. Serial dilutions were performed to obtain AMP concentrations ranging from 512 µg/mL to 0.125 µg/mL. Meanwhile, a 3 mg/mL fluorescamine solution was prepared by dissolving fluorescamine powder in acetone, and 50 µL were added to the wells. A fluorescamine control (with 150 µL of water and 50 µL of fluorescamine solution) and a water control (with 200 µL of ultrapure water) were made. Finally, the fluorescence of the samples was read on a Synergy MX microplate reader (BioTek, Vermont, USA) at the i3S Biointerfaces and Nanotechnology scientific platform with 400/460 nm excitation-emission wavelengths.

AMP concentrations in the AMP-NP samples were then determined based on the calibration curve by the same procedure. The samples were diluted 1:4 to guarantee that fluorescence values were within the range of the calibration curve. AMP immobilization efficiency (IE %) was determined by dividing the amount of AMP that remains immobilized on the particles after the last washing step of the preparation protocol by the total added amount (equation 1).

$$\mathrm{IE}\ \% = \frac{\mathrm{m(AMP)_{immobilized}}}{\mathrm{m(AMP)_{added}}} \times 100\ \% \qquad \text{(Equation 1)}$$

2.7. Shelf stability assessment

The DLS characterization of the AMP-NP samples was carried out after a period of 10 weeks in storage at 4 ºC and 20 weeks frozen at -80 ºC to evaluate the stability of the nanoconjugate over time in different conditions.

3. Antimicrobial activity

3.1. Microorganisms and growth conditions

Microorganisms tested in this study were *Staphylococcus aureus* (*S. aureus*) ATCC 25923 and *Pseudomonas aeruginosa* (*P. aeruginosa*) ATCC 27853. Bacteria were grown on tryptic soy agar (TSA) plates, Mueller-Hinton Broth (MHB) (Sigma-Aldrich, Missouri, USA) and tryptic soy broth (TSB) (Merck).

3.2. Minimum inhibitory concentration (MIC) and minimum bactericidal concentration (MBC) assay

The antimicrobial activity of the formulated AMP-NPs was obtained against *S. aureus* and *P. aeruginosa* by minimum inhibitory concentration (MIC) and minimum bactericidal concentration (MBC) assessment. This assay was done through the standard broth microdilution on microtiter plates, as described by (Wiegand et al., 2008). The samples were adjusted according to AMP concentration by dilution in ultrapure water. Controls of bare PLGA-PEG NPs contained the same NP concentration as each AMP-NP sample. 25 µL of diluted sample were added to 75 µL of inoculum adjusted to 2.0×10^5 CFU/mL in MHB on the wells of a round-bottom polypropylene 96-well plate (Corning Incorporated, New York, USA). This plate allows to easily identify bacterial growth and prevents bacterial adhesion to the walls of the well. A positive control with 75 µL of inoculum and 25 µL of ultrapure water, a negative control with 75 µL of MHB and 25 µL of ultrapure water, and a negative control with 25 µL of each NP sample with 75 µL of MHB were also made.

Bacteria were prepared by spreading stock solution in a TSA plate, leaving to grow overnight at 37 ºC, and subsequently inoculating one colony in 5 mL of MHB and incubating overnight at 150 rpm and 37 ºC. To adjust inoculum concentration, the bacterial suspension was recovered by centrifugation (2700 rpm, 10 min), washed in PBS, and after a new centrifugation it was resuspended in 5 mL of PBS. Optical density (OD) was measured in an Ultrospec 10 Cell Density Meter (Biochrom, Cambridge, UK) at 600 nm, and inoculum concentration was adjusted in MHB or simulated wound fluid (SWF) according to known correlations between OD and colony forming units (CFUs) for each bacterial strain (6.1 OD_{600} – 1.2×10^9 CFU/mL for *S. aureus* and 2.6 OD_{600} – 2.25×10^9 CFU/mL for *P. aeruginosa*). Bacterial inocula were serially diluted in PBS and plated for CFU counting confirmation.

SWF was composed of 50 % fetal bovine serum (FBS) (Sigma) and 50 % peptone water with 0.9 % sodium chloride (NaCl) in 0.1 % peptone (Sigma), as described by (Price et al., 2016). The peptone water was prepared fresh for each experiment and mixed with FBS after filtering with a 0.22 µm filter (Fisherbrand, Pennsylvania, USA).

The plate was left to incubate at 37 ºC for 18-24 hours and microbial growth in the bottom of the wells was evaluated by direct observation. The MIC of the AMP-NP conjugate was determined as the lowest AMP concentration with an absence of visible growth. The content of the wells without visible growth was then serially diluted to a magnitude of 10^{-7} in PBS in 96-well suspension plates (Sarstedt, Nümbrecht, Germany), and the contents were plated in TSA plates. CFUs were counted after an overnight incubation at 37 ºC to determine the minimum bactericidal concentration (MBC), the lowest AMP concentration that causes a viability reduction of ≥ 99.9 % of the initial inoculum. All the procedures in this section were done in a sterile environment with sterile equipment and reagents.

3.3. Time-kill assay in growth medium

Killing kinetics were determined for *S. aureus* and *P. aeruginosa* in MHB through a time-kill assay. Bacteria inocula were prepared as above and the AMP was used as control for these assays. A final volume of 180 µL was used for incubation in the wells. For that, MSI-78(4-20) dilutions were prepared in a solution of 0.01 % acetic acid (Panreac, Barcelona, Spain) and 0.2 % bovine serum albumin (BSA) (Sigma) to prevent AMP aggregation. Bare NPs were also used as control. As soon as the plate was ready, it was placed in an incubator at 37 ºC and removed at specific timepoints to collect aliquots of 30 µL from the wells. Appropriate serial dilutions were made for each timepoint with PBS and the contents plated in TSA plates. The plates were incubated overnight at 37 ºC and CFUs were counted to determine bacterial concentrations in the wells.

3.4. Minimum biofilm eradication concentration (MBEC) assay

The ability of AMP-NPs to disrupt pre-formed biofilm was tested on the model organism *P. aeruginosa* through the minimum biofilm eradication concentration (MBEC) assay. After plating the bacterium on a TSA plate and leaving to grow overnight at 37 ºC, 4-5 large colonies were inoculated in 100 mL of TSB and incubated overnight at 150 rpm and 37 ºC. In the following day, OD was measured at 600 nm and the inoculum adjusted to 10^7 CFU/mL in TSB. Serial dilutions in PBS and plating were performed for CFU counting confirmation.

150 µL of inoculum were added to a 96-well MBEC biofilm inoculator plate (Innovotech, Edmonton, Canada) and it was incubated at 110 rpm and 37 ºC to allow biofilm to form in the surface of the pins. To preserve humidity, the outermost wells were filled with ultrapure water and the plate was stored inside a box with wet paper towels. The plate was incubated for a total of 48 hours, with the content of the wells being replaced for fresh medium after 24 hours.

After biofilm growth, a new 96-well round-bottom polypropylene plate was used to prepare AMP and AMP-NP dilutions with 0.01 % acetic acid and 0.2 % BSA solution and ultrapure water, respectively. 50 µL of sample were added to 150 µL of MHB and the MBEC lid was transferred to the new plate. A positive biofilm control was made with 50 µL of ultrapure water and 150 µL of MHB, and sterility controls were made with 50 µL of 0.01 % acetic acid and 0.2 % BSA solution or ultrapure water and 150 µL of MHB. The plate was incubated at 37 ºC and 110 rpm overnight.

Biofilm was quantified by staining with crystal violet dye. After incubation with NPs and AMP, the pins were washed three times with PBS and left overnight to dry. The pins were submerged for 10 minutes in 200 µL of a 0.4 % crystal violet (Sigma-Aldrich) solution in water. The solution was removed and the pins were left to dry for 10 minutes, after which they were washed with ultrapure water until no dye was visible in the washing water (three to five times). 210 µL of dimethyl sulfoxide (DMSO) (Thermo Fisher Scientific, Massachusetts, USA) were added to the wells to dissolve the dye and sonication was performed when necessary to achieve complete dissolution (ultrasonic cleaner, VWR). The absorbance of the plate was measured at 595 nm in a microplate reader (Powerwave XS, BioTek).

4. Statistical analysis

Statistical analysis was performed using GraphPad Prism version 9.0.2 for Mac OS X (GraphPad Software, California, USA). Ordinary one-way analysis of variance (ANOVA) with Dunnett's multiple comparisons test was used to compare multiple groups of data to a control. Values are presented as mean ± standard deviation (SD). Statistical significance is indicated as *$p \leq 0.05$, **$p \leq 0.01$, ***$p \leq 0.001$ and ns (not significant).

Results and discussion

1. AMP-NP characterization

1.1. Dynamic light scattering (DLS) and laser Doppler anemometry

Initially, five NP samples were produced: PLGA-PEG NPs, NPs with different PLGA-PEG: PLGA-PEG-Mal mass ratios with AMP – 9:1 (10%Mal-AMP), 8:2 (20%Mal-AMP) and 6:4 (40%Mal-AMP) –, and PLGA-PEG NPs with AMP as an adsorption control (AMPads), using the same amount of AMP as 40%Mal-AMP (table 5). A 1:2.5 Mal:AMP molar ratio was used for AMP functionalization based on previous optimization.

Table 5 - Legend and composition of the samples produced with this protocol.

Name	NP composition (mass ratio)
PLGA-PEG	PLGA-PEG
AMPads	PLGA-PEG + AMP
10%Mal-AMP	9 PLGA-PEG : 1 PLGA-PEG-Mal + AMP
20%Mal-AMP	8 PLGA-PEG : 2 PLGA-PEG-Mal + AMP
40%Mal-AMP	6 PLGA-PEG : 4 PLGA-PEG-Mal + AMP

The size distribution and surface charge of the samples is displayed on figure 9. Except for the adsorption control, all samples have around 100 nm of size and low polydispersity (PdI < 0.2). Although the presence of immobilized AMP causes a noticeable increase in size in comparison to bare NPs (96 nm for PLGA-PEG, 138 nm for 10%Mal-AMP, 122 nm for 20%Mal-AMP, and 119 nm for 40%Mal-AMP), this difference is not significant. On the other hand, AMPads has a significant increase in size (160 nm), which can be attributed to the adsorption of multiple layers of AMP or a reorganization of the NP structure upon AMP interaction. This sample also has the most inconsistent size, likely due to the random nature of adsorption as opposed to covalent binding.

As for surface charge, PLGA-PEG NPs have a negative ZP (-2.83 mV) due to the presence of carboxylic groups in PLGA. AMP addition causes a transition to positive values due to the cationic nature of these peptides, also reported for other PLGA NPs with immobilized AMPs (Vijayan et al., 2019). ZP values were 3.6 mV for 10%Mal-AMP, 6.34 mV for 20%Mal-AMP, and 8.67 mV for 40%Mal-AMP. It's possible to identify a trend of growing ZP values with increasing percentages of Mal-modified

polymer (with the highest charge for 40%Mal-AMP), which suggests greater amounts of immobilized AMP. ZP has been correlated with AMP concentrations in other cases of AMP functionalization to NPs (Boge et al., 2017). Again, AMPads had an inconsistent behavior and the lowest charge of all AMP-modified samples at 2.37 mV, highlighting the effectiveness of the maleimide-thiol reaction compared to adsorption.

NP physical properties such as size, shape and charge can influence their skin absorption (Manikkath et al., 2018). Loaded PLGA NPs of 50 nm and 100 nm showed passive skin permeability in an *ex vivo* rat skin model, and while 100 nm NPs caused a significant effect, 50 nm NPs led to a higher drug accumulation and permeation through the skin, with absorption occurring mainly through hair follicles (Takeuchi et al., 2017). Regardless, the presence of the hydrophilic PEG on the NP surface could also influence this behavior. Copolymeric NPs of polylactic acid (PLA) and PEG (100 nm and -33 < ZP < -3.5) were shown to have higher absorption in intact porcine skin with the increase in PEGylation (Lalloz et al., 2019). While skin absorption would not be a concern for application in open wounds or impaired skin – where the stratum corneum (SC) is disrupted – literature suggests PLGA-PEG NPs could also permeate the skin layers of surrounding tissue and prevent infection from spreading. Because PLGA NPs are biodegradable and biocompatible, their diffusion through the skin is unlikely to cause any adverse effects.

Besides preventing aggregation and increasing stability, the positive charge of AMP-NPs could enhance their permeation through the negatively-charged SC, the outermost skin layer, which offers the greatest barrier to drug absorption. Higher stability and diffusion through the SC has been shown for cationic liposomes when compared to anionic ones (Manosroi et al., 2004), though the opposite has also been found. Thus, the influence of surface charge on NP skin absorption is still poorly understood. The dispersion vehicle, duration of exposure, and use of techniques such as ultrasound and iontophoresis could also enhance absorption (Manikkath et al., 2018).

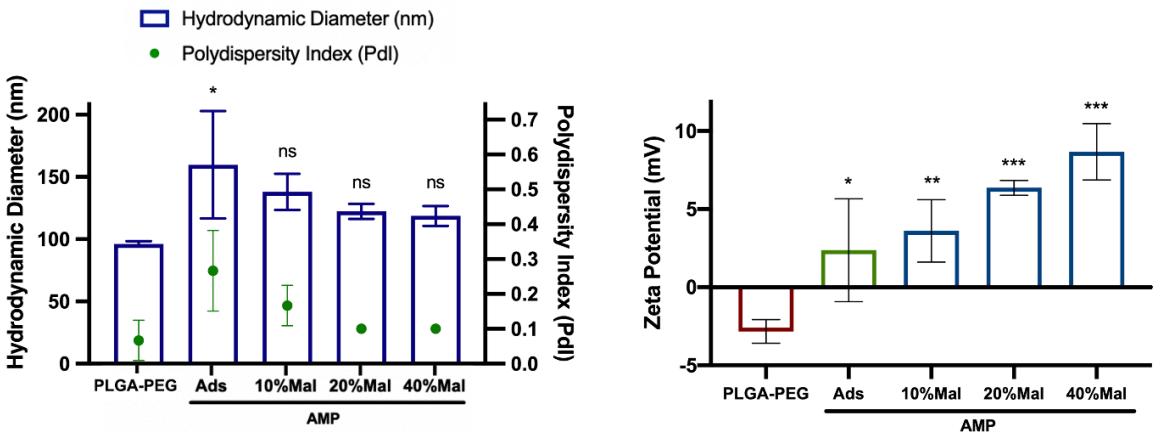

Figure 9 - (A) Hydrodynamic diameter and PdI and (B) ZP of bare PLGA-PEG NPs and AMP-modified NPs. Values are presented as mean ± SD (n=3). Ordinary one-way ANOVA with Dunnett's multiple comparisons test was used to compare all samples to the NP control. Statistically significant differences are indicated as *$p \leq 0.05$; **$p \leq 0.01$; ***$p \leq 0.001$ and ns (not significant).

1.2. Transmission electron microscopy (TEM)

The morphology of NPs was observed through TEM. From the images obtained (figure 10), it's possible to observe that both unmodified and AMP-functionalized PLGA-PEG NPs have a spherical shape without visible aggregation. Therefore, AMP conjugation to the NP surface does not appear to affect NP morphology. These results are consistent with the ones obtained from DLS and NTA.

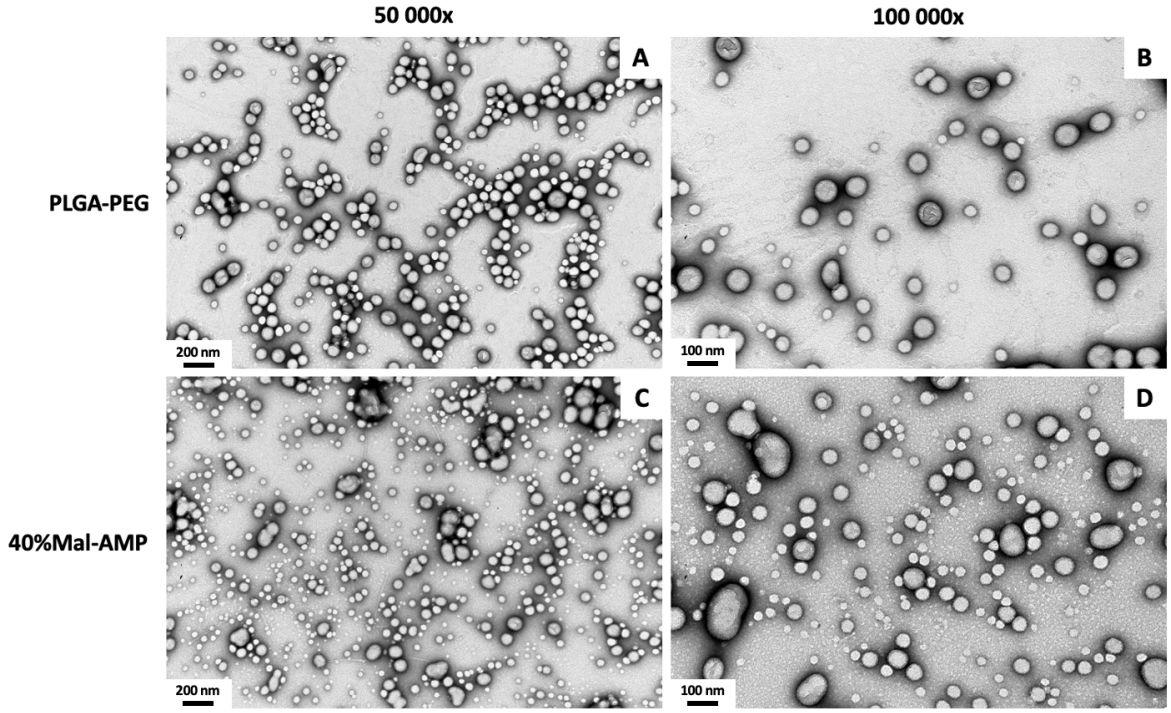

Figure 10 - TEM images of bare PLGA-PEG NPs and AMP-modified NPs (40%Mal-AMP) at 50 000x (A and B, respectively) and 100 000x magnification (C and D, respectively).

1.3. Fourier-transform infrared (FTIR) spectroscopy

FTIR was performed to characterize the NPs and confirm the presence of AMP in Mal-AMP NPs, using 40%Mal-AMP and respective controls (figure 11). Evident PLGA peaks include C=O stretching at 1762.6 cm^{-1}, C-H stretching at 2885-3010 cm^{-1}, O-H stretching at 3455-3500 cm^{-1}, C-O stretching at 1186-1089 cm^{-1}, and CH_2 bending peaks at 850-1450 cm^{-1} (Singh et al., 2014). The C-O and C-H bands are also characteristic of PEG, as well as C-O-C stretching at 1089 cm^{-1} (Deygen & Kudryashova, 2016). In the 40%Mal-AMP sample, three additional bands are present (highlighted in figure 12): amide A (N-H stretching) at 3300 cm^{-1}, amide I (C=O stretching) at 1600-1690 cm^{-1} and amide II (C-N stretching and N-H bending) at 1480-1575 cm^{-1}, characteristic of amino acids (Kong & Yu, 2007).

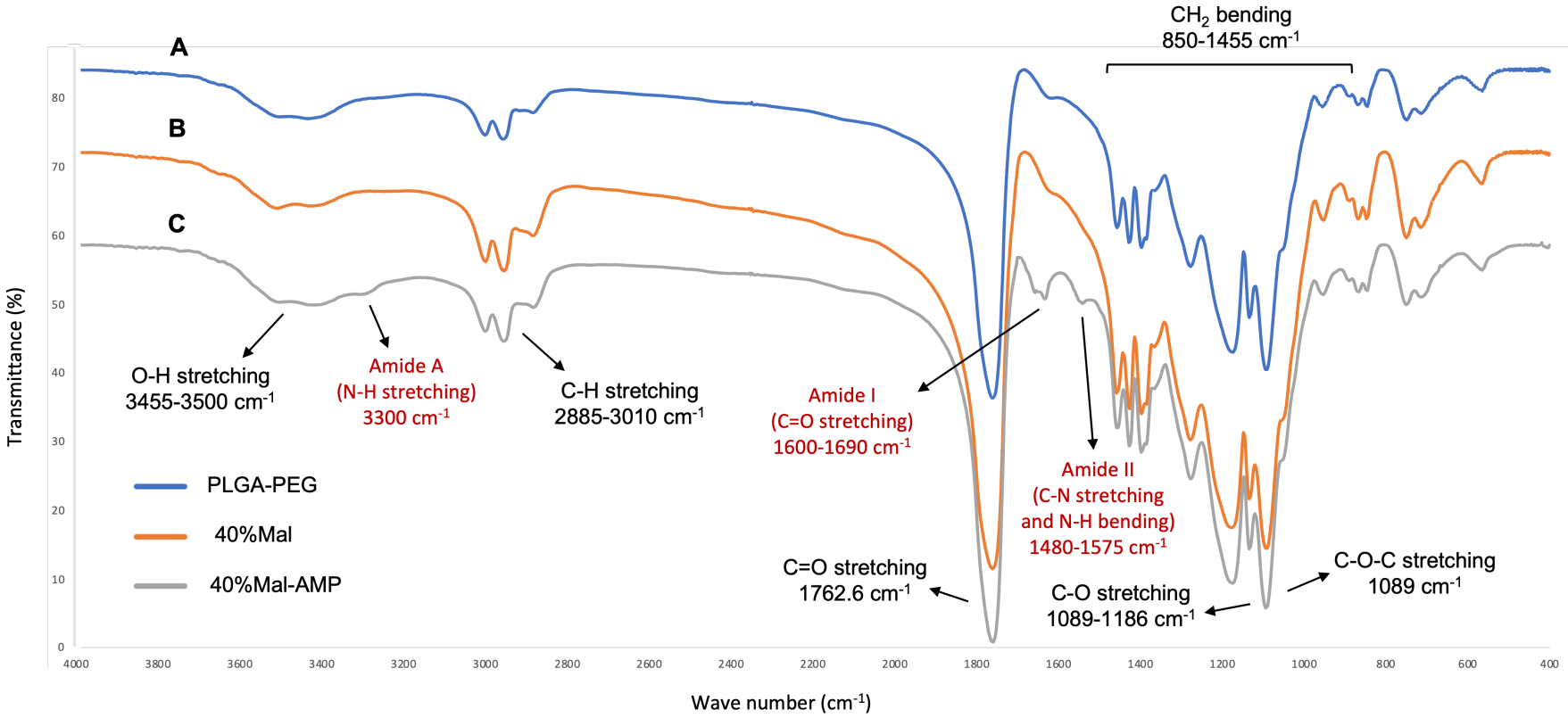

Figure 11 - FTIR spectra of (A) PLGA-PEG NPs, (B) bare NPs produced with 40% PLGA-PEG-Mal (without AMP), and (C) 40%Mal-AMP NPs (with AMP). Marked peaks (from left to right) detectable in all samples are: O-H stretching at 3455-3500 cm^{-1}, C-H stretching at 2885-3010 cm^{-1}, C=O stretching at 1762.6 cm^{-1} from ester groups, CH_2 bending at 850-1455 cm^{-1}, and C-O stretching at 1089-1186 cm^{-1} characteristic of PLGA polymer chain. In addition to C-O and C-H bands, PEG is also detected by C-O-C stretching from ether groups at 1089 cm^{-1}. In the spectrum corresponding to 40%Mal-AMP, three additional peaks distinctive of amino acids are marked in red (from left to right): amide A (N-H stretching) at 3300 cm^{-1}, amide I (C=O stretching) at 1600-1690 cm^{-1}, and amide II (C-N stretching and N-H bending) at 1480-1575 cm^{-1}.

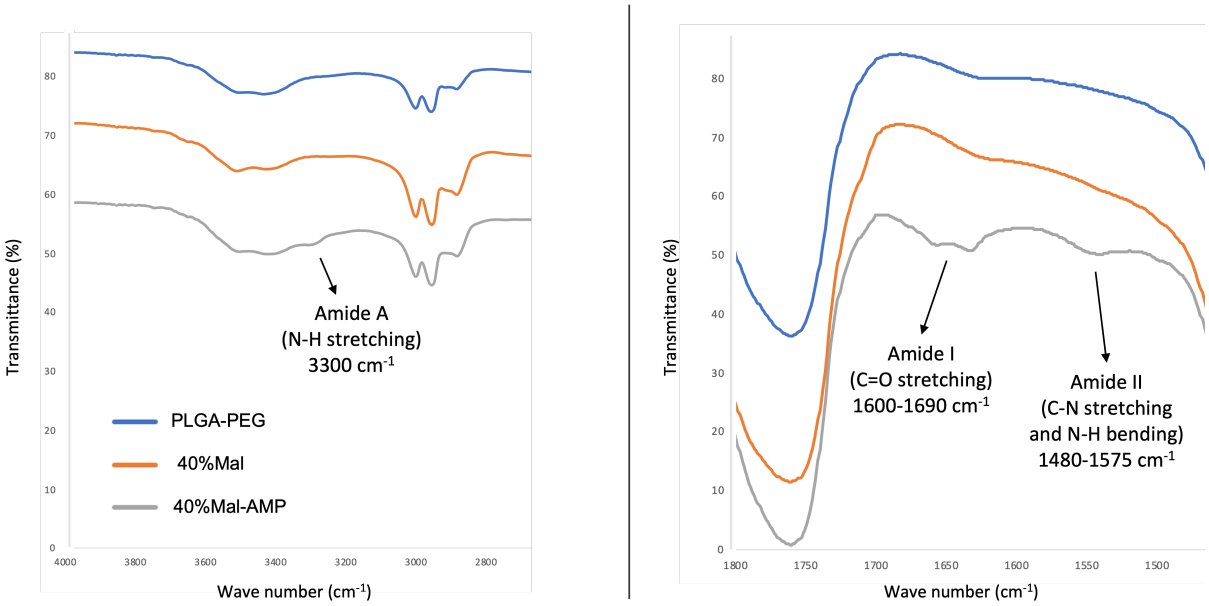

Figure 12 - Regions of the FTIR spectra where AMP bands can be identified. Three additional bands are present in the 40%Mal-AMP spectrum due to AMP functionalization: amide A (N-H stretching) at 3300 cm^{-1}, amide I (C=O stretching) at 1600-1690 cm^{-1}, and amide II (C-N stretching and N-H bending) at 1480-1575 cm^{-1}.

1.4. Nuclear magnetic resonance (NMR) spectroscopy

H^1-NMR spectroscopy was done to assess covalent binding of the AMP to NPs. Mal has a clear peak in the aromatic region at 6.728 ppm, corresponding to the hydrogen atoms surrounding the double bond (Chemical Book, n.d.). After AMP conjugation via thiol groups, the molecule's antiaromaticity is disrupted due to the breakage of the double bond (Roux et al., 1997), causing loss of the antiaromatic ring current and downfield shift of ^1H nuclei. In this case, there is a clear reduction of the Mal peak from PLGA-PEG-Mal polymer to bare 40%Mal NPs due to decreased Mal concentration. This reduction is further accentuated in 40%Mal-AMP (figure 13), which indicates the maleimide-thiol reaction between the AMP and Mal, indirectly confirming AMP covalent conjugation.

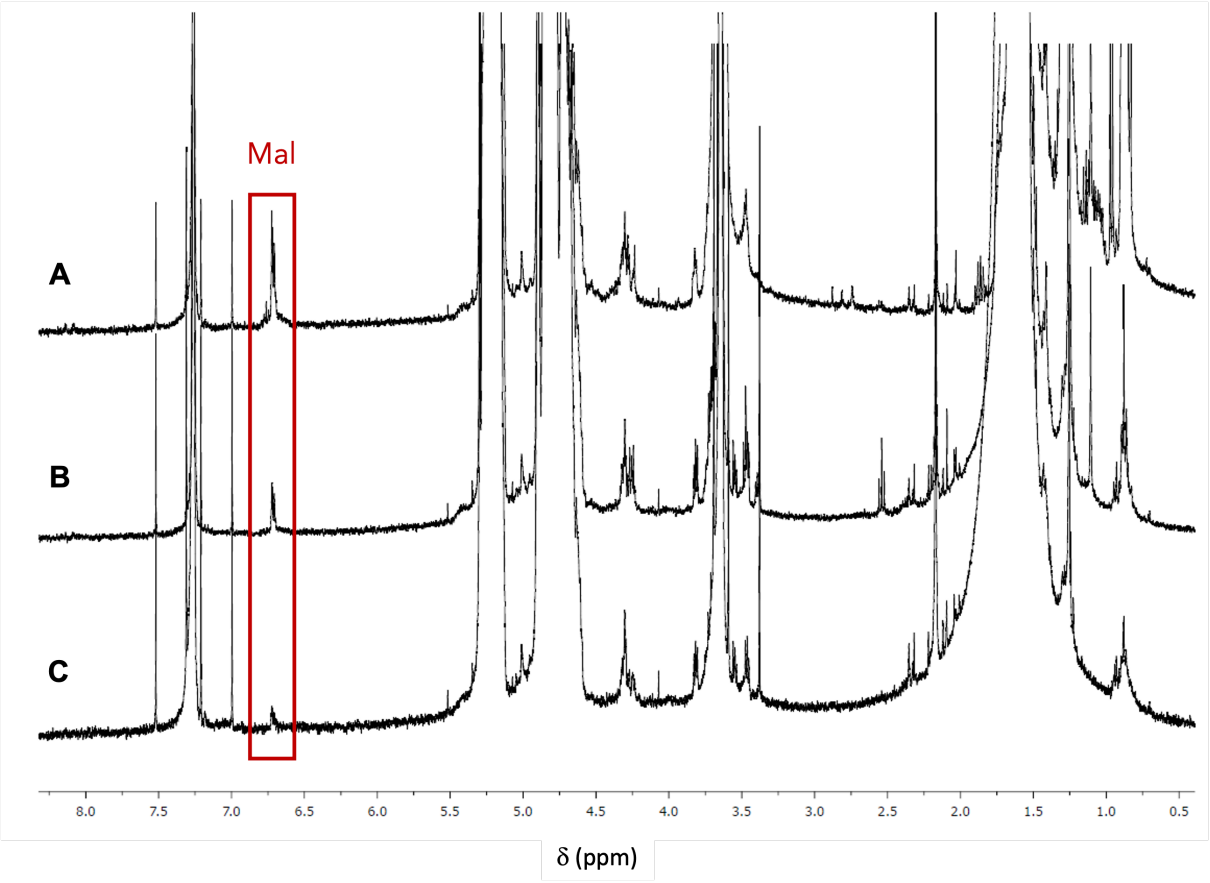

Figure 13 - ^{1}H NMR spectra (400 MHz, $CDCl_3$) of (A) PLGA-PEG-Mal polymer, (B) bare NPs produced with 40% PLGA-PEG-Mal (40%Mal), and (C) 40%Mal-AMP NPs. AMP signals from the peptide could not be detected in the ^{1}H-NMR spectrum (neither in $CDCl_3$ nor in DMSO-d6) due to the very small amounts of peptide linked. However, it was possible to observe the disappearance of the signal corresponding to the maleimide protons of the NPs (6.728 ppm, identified with a red rectangle) on the spectrum corresponding to 40%Mal-AMP, which indirectly indicates the conjugation of AMP to NPs.

1.5. Fluorescamine assay (AMP quantification)

Direct AMP quantification was done through a fluorescamine assay. Average AMP concentrations were 165.5 µg/mL for AMPads, 155 µg/mL for 10%Mal-AMP, 206 µg/mL for 20%Mal-AMP, and 326 µg/mL for 40%Mal-AMP. It was confirmed that adsorption led to inconsistent amounts of AMP and, using this sample as a comparison, only 40%Mal-AMP had a significantly increased amount of AMP (figure 14). These data confirm that higher PLGA-PEG-Mal ratios used in NP production led to higher amounts of immobilized AMP.

Average IE values were 49.0 %, 32.6 % and 25.8 % for 10%Mal-AMP, 20%Mal-AMP and 40%Mal-AMP, respectively. Due to the 1:2.5 Mal-AMP ratio used in NP production, the theoretical IE threshold is 40 %. The higher value obtained for 10%Mal-AMP suggests part of the AMP immobilized on this sample is bound by non-covalent forces and is likely to take place in the other samples as well, although to a smaller extent. As expected, AMPads had the lowest IE at 13.1 %.

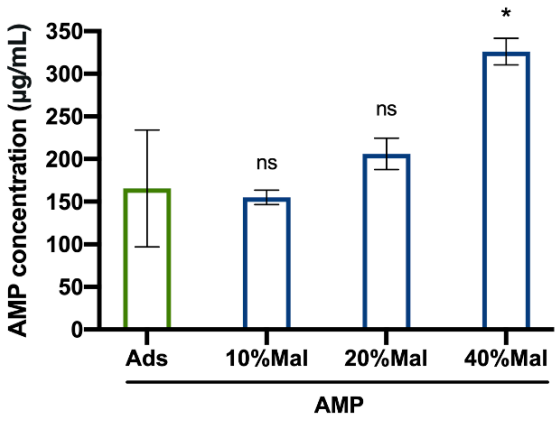

Figure 14 - Results of AMP quantification in the NP samples. Values are presented as mean ± SD (n=2). Ordinary one-way ANOVA with Dunnett's multiple comparisons test was used to compare all samples to AMPads. Statistically significant differences are indicated as *p ≤ 0.05; **p ≤ 0.01; ***p ≤ 0.001 and ns (not significant).

1.6. Shelf stability assessment

DLS characterization of the NP samples was repeated after periods in storage to assess their stability at 4 ºC and -80 ºC (table 6). After 10 weeks at 4 ºC, there was a considerable increase in size and PdI for 40%Mal-AMP only. On one hand, this behavior is unexpected, as the higher surface charge of this sample would increase repulsion between NPs and prevent aggregation. On the other, ZP results show a marked decrease during storage, which could be due to AMP or NP degradation – with indirect removal of bound AMP. Although this could theoretically favor aggregation, the size and charge of the other samples (PLGA-PEG and AMPads) did not vary significantly. Therefore, this behavior is probably a result of other interactions between covalently-linked AMP, such as hydrophobic interactions, which lead to NP aggregation. As stated, MSI-78 has been shown to form dimers in solution (Porcelli et al., 2006), which might be preserved to some extent in MSI-78(4-20).

At -80 ºC, there was considerable aggregation for control PLGA-PEG NPs, proven by a dramatic increase of size and PdI. AMP samples were stable, with only a slight decrease of size for both AMPads and 40%Mal-AMP and of PdI for AMPads. A reduction of surface charge was obtained for 40%Mal-AMP similar to the case at 4 ºC, which could also be explained by AMP or NP degradation. Regardless, these experiments were done with only one NP batch and must be repeated to confirm results.

Table 6 - Results of DLS analysis of the same NP batch before and after storage for 10 weeks at 4 ºC and 20 weeks at -80 ºC.

	Sample	Hydrodynamic diameter (nm)		Polydispersity index		Zeta potential (mV)	
		Before	After	Before	After	Before	After
4 ºC	PLGA-PEG	96.8 ± 0.7	95.8 ± 0.6	0.1	0.1	-3.0 ± 0.6	-3.1 ± 0.2
	AMPads	166.9 ± 3.2	156.3 ± 1.4	0.2	0.2	-1.3 ± 1.5	-1.7 ± 0.9
	40%Mal-AMP	120.0 ± 2.8	172.6 ± 2.1	0.1	0.3	8.8 ± 0.7	4.7 ± 0.6
-80 ºC	PLGA-PEG	98.1 ± 0.3	394.6 ± 5.2	0.1	0.6	-3.5 ± 1.3	-1.4 ± 0.3
	AMPads	198.8 ± 14.3	175.0 ± 1.6	0.4	0.3	3.3 ± 0.7	2.7 ± 0.4
	40%Mal-AMP	125.9 ± 1.3	121.5 ± 0.3	0.1	0.1	10.4 ± 0.6	5.8 ± 0.3

2. Antimicrobial activity

2.1. Minimum inhibitory concentration (MIC) and minimum bactericidal concentration (MBC) assay

Antimicrobial activity of the AMP when grafted to NPs was evaluated against *S. aureus* and *P. aeruginosa* in growth medium and SWF by determination of MIC and MBC. Due to having the highest concentration of immobilized AMP, 40%Mal-AMP was selected to further study antimicrobial activity using different AMP concentrations. From this point forward, this sample will be referred to as AMP-NPs and MSI-78(4-20) as AMP.

In order to interpret results, it is important to note the structural differences of Gram-positive and Gram-negative envelopes (Silhavy et al., 2010). The outermost layer of Gram-negative bacteria is an outer membrane composed of phospholipids in the inner leaflet and glycolipids such as LPS in the outer leaflet. Its main function is protection and it's responsible for the greater antibiotic resistance of these bacteria. Access is especially difficult for large hydrophilic molecules due to LPS packing and limited diffusion through porins. The outer membrane is followed by the periplasm compartment, which contains a thin peptidoglycan cell wall (1.5-10 nm) and a high concentration of proteins and enzymes, followed by the phospholipid bilayer that comprises the inner or cell membrane. Gram-positive organisms, on the other hand, lack the stabilizing outer membrane, which is compensated by a thick layer (30-100 nm) composed largely of peptidoglycan combined with TAs. A simplified scheme of Gram-positive and Gram-negative bacterial envelopes can be seen on figure 15.

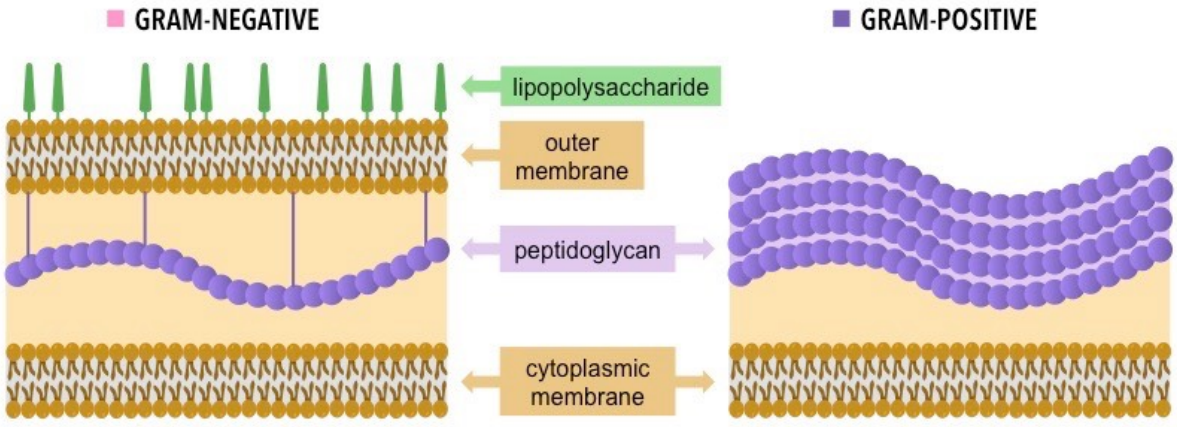

Figure 15 - Scheme of the major structural differences between Gram-negative and Gram-positive bacterial envelopes (Gram Staining | BioNinja, n.d.).

2.1.1. MIC and MBC in growth medium

In growth medium, both AMP and AMP-NPs were highly effective against *S. aureus* and *P. aeruginosa*, proven by low MIC and MBC values (table 7). Additionally, bactericidal activity was achieved with only 2-fold of inhibitory concentrations, which highlights the killing efficiency of MSI-78(4-20) and is in agreement with its bactericidal mechanism. MIC and MBC values of the AMP were slightly higher than previously reported (Monteiro et al., 2015), which is probably a result of different quantification methods being used. Both AMP and AMP-NPs were more effective against the Gram-negative *P. aeruginosa* than the Gram-positive *S. aureus*. This difference was also seen for the same AMP and the parent peptide (MSI-78) in previous work by our group with Gram-positive organisms MRSA and *S. epidermidis* (Monteiro et al., 2015).

This trend, also shared with other membrane-disrupting AMPs, can be explained by the thick Gram-positive cell wall preventing access to the cell membrane. In contrast, the exposed Gram-negative outer membrane may be disrupted by AMPs, leaving only the thin peptidoglycan layer as a barrier to the cell membrane. Besides, cationic peptides have been shown to cross the outer membrane by binding LPS or lipid A and displacing Mg^{2+} through a self-promoted pathway (Moore et al., 1986). Still, there is considerable debate regarding the role of the cell wall in the effectiveness of AMPs, in whether they decrease AMP concentrations at the cell membrane or act as a sponge by further directing them to the membranes (Malanovic & Lohner, 2016). While peptidoglycan is relatively porous to small molecules, anionic TAs can electrostatically bind AMPs. On the other hand, conventional antibiotics and currently approved AMPs are generally less effective against Gram-negative organisms, where the protective effect of the outer membrane is likely the determining factor.

The surface charge of bacteria can also elucidate the higher efficacy against *P. aeruginosa*. The electrophoretic mobility (EPM) of the bacterial strains used in this work has been determined elsewhere as -0.551 µm cm $V^{-1} s^{-1}$ for *S. aureus* and -0.970 µm cm $V^{-1} s^{-1}$ for *P. aeruginosa*, using neutral pH and standard growth conditions (Bayer & Sloyer, 1990). The more negative EPM of *P. aeruginosa* might lead to stronger electrostatic attraction to AMPs and the higher efficiency towards this species.

In respect to AMP conjugation to NPs, there was no difference of MIC or MBC between free and NP-bound AMP against *S. aureus*, meaning the AMP maintained its effectiveness with a MIC of 16-32 µg/mL and an MBC of 32-64 µg/mL. For *P. aeruginosa*, there was a 4-fold reduction in AMP effectiveness, from a very low MIC and MBC of 1-2 µg/mL and 2-4 µg/mL for the AMP to 8-16 µg/mL and 16-32 µg/mL, respectively, for AMP-NPs. This could be a result of immobilization altering AMP interaction with the outer membrane, possibly by decreasing binding to LPS. The size of NPs could also prevent crossing the outer membrane and cell wall and consequently reaching the cell membrane.

Similar loss of effectiveness has been reported for other covalently immobilized AMPs. For instance, (Wu et al., 2017) found that the MIC of cecropin P1 against *E. coli* increased considerably when immobilized on silica NPs through Mal-PEG-(N-Hydroxysuccinimide) linkers. The authors attribute the effect to the presence of the linker preventing AMP interaction with the bilayers. Metallic NPs are often covalently combined with AMPs, but because they are antibacterial at low concentrations, conjugation usually results in decreased MIC values and it's not possible to discern the impact of immobilization on antimicrobial activity.

2.1.2. MIC and MBC in simulated wound fluid (SWF)

Antimicrobial activity was also measured in SWF that mimics the natural composition of the wound environment, prepared with equal parts FBS and peptone water. Final SWF composition includes proteins and enzymes (with BSA as its main component), electrolytes, lipids, carbohydrates, peptic digest of animal tissue, and other undefined constituents. FBS was not heat-inactivated to preserve the structure and activity of its components.

Results in this medium were more heterogeneous than in standard growth medium, which led to wider MIC and MBC ranges for most conditions. Curiously, there was an increase in AMP effectiveness against *S. aureus*, to a MIC and MBC of 4-16 µg/mL and 8-16 µg/mL, respectively. AMP-NP activity was maintained, with both MIC and MBC at 16-64 µg/mL. The opposite effect was seen for *P. aeruginosa*, with MIC and MBC of the AMP increasing to 8-32 µg/mL and 16-64 µg/mL, respectively. AMP-NPs also lost activity against this bacterium, with the MIC increasing to 128-256 µg/mL. Bactericidal activity of AMP-NPs was obtained in some assays for an AMP concentration of 256 µg/mL but could not be consistently reproduced. Results are collected in table 7. As a whole, results show there was a reversal of the trend observed in growth medium by making the AMP and AMP-NPs more effective towards the Gram-positive *S. aureus* in SWF.

Table 7 - MIC and MBC values of AMP and AMP-NPs against *S. aureus* and *P. aeruginosa* determined in standard growth medium and SWF. Results from three independent experiments.

Medium		Microorganisms			
		S. aureus (ATCC 25923)		*P. aeruginosa* (ATCC 27853)	
		MIC (µg/mL)	MBC (µg/mL)	MIC (µg/mL)	MBC (µg/mL)
Growth medium	AMP	16 - 32	32 - 64	1 - 2	2 - 4
	AMP-NPs	16 - 32	32 - 64	8 - 16	16 - 32
Simulated wound fluid (SWF)	AMP	4 - 16	8 - 16	8 - 32	16 - 64
	AMP-NPs	16 - 64	16 - 64	128 - 256	256 - >256

Due to the structural complexity of SWF, interpretation of results is not as straightforward as in growth medium. The observed differential effect cannot be explained simply by proteins and other SWF elements binding and limiting AMP activity, as that would require loss of activity for both bacterial strains. Likewise, differences in pH of both media could also contribute but not fully account to these results. The pH of MHB and SWF was measured at 7.09 and 7.72, respectively. For a peptide rich in basic residues such as MSI-78(4-20), an increase in pH will lead to a lower overall charge. This could theoretically lead to weaker electrostatic interactions with bacterial membranes and consequent reduced activity. Such phenomenon could contribute to the loss of activity against *P. aeruginosa*. NP degradation likely didn't play a part in these differences, as slightly acidic or basic media have been shown to not significantly affect PLGA degradation rates (Y. Xu et al., 2017).

Instead, this could be a result of different degrees of affinity of MSI-78(4-20) to Gram-positive and Gram-negative bacterial components as well as to elements of the fluid. We hypothesize that in this medium the AMP has greatest affinity to Gram-positive peptidoglycan and TAs, followed by serum

proteins and other SWF elements, and finally outer membrane lipids and LPS of Gram-negative bacteria. Detailed studies of AMP affinity and mechanisms will have to be carried out to confirm this.

(Thapa, Winther-Larsen, et al., 2020) studied the stability of multiple peptides in SWF and found that all were considerably degraded after 1 day at 37 ºC (60-90 %) and completely degraded after 5 days, though antimicrobial activity in SWF was not assessed. This raises the question of whether degradation of MSI-78(4-20) takes place before its bactericidal activity. Additionally, the activity of multiple AMPs derived from centrocin 1 was assessed in 50 % SWF against *S. aureus* and *P. aeruginosa*, with all peptides being less effective when compared to standard growth medium and some not having any effect at the highest concentration tested (Björn et al., 2012). A similar behavior took place with PXL150 when tested against *S. aureus* in SWF, in which despite over 10 times reduction in activity, reasonable bactericidal activity was still obtained (Myhrman et al., 2013). It's important to mention that these studies used heat-inactivated SWF, which could degrade some of the serum elements and prevent them from interacting with AMPs.

2.2. Time-kill assay in growth medium

A time-kill assay was done to evaluate the killing kinetics of AMP and AMP-NPs in growth medium against *S. aureus* and *P. aeruginosa*. The timepoints used were based on preliminary experiments that determined the earliest timepoint at which the previously determined MBC values caused complete death.

Treatment with AMP caused complete death at 6-8 hours for *S. aureus* and at 30 minutes - 1 hour for *P. aeruginosa* (figures 16A and 16B). This is in accordance with values obtained for the parent peptide MSI-78 (2 hours for *S. aureus* and 10 minutes for *P. aeruginosa* at 4× MIC) (Ge et al., 1999). Other AMPs have been put to the test against both bacteria, with varying results. (Kwon et al., 2019) tested various membrane-active truncated AMPs based on P5, a hybrid of cecropin A and magainin-2. Despite obtaining lower MIC values for *S. aureus*, activity in general was faster against *P. aeruginosa* (5 minutes as opposed to 6 hours at 2× MIC for *S. aureus*). A small yet opposite effect was seen with melectin, an AMP derived from bee venom (Ko et al., 2020). After 5 minutes, there was over 90 % death for *S. aureus* and 80 % for *P. aeruginosa*. The variability of relative killing speed between Gram-positive and Gram-negative bacteria may be due to different affinities of each peptide sequence to the specific elements present in their outer layers, as explained above. For MSI-78(4-20), at least regarding activity in growth medium, it appears that the protective effect of the thicker peptidoglycan wall of *S. aureus* is prevalent both when it comes to potency and killing kinetics.

While AMP loading would likely lead to delayed kinetics due to antimicrobial activity being dependent on NP degradation, the impact of surface immobilization is harder to predict and hasn't been studied extensively. Remarkably, AMP conjugation to NPs improved killing kinetics for both strains, leading to complete death at 1-2 hours for *S. aureus* and at 15 minutes for *P. aeruginosa* (figures 16C and 16D), with the difference being particularly significant for *S. aureus*. As expected, PLGA-PEG NPs at the same NP concentration had no impact on bacterial growth.

The killing kinetics of AMPs AP114 and DPK-060 have been studied against *S. aureus* when loaded onto cubosomes (Boge et al., 2016). NPs alone had no effect on bacterial growth and AMP-loaded cubosomes behaved similarly to the unformulated peptides, which was credited to a burst release taking place and increasing the amount of AMP free to exert action. The same AMPs were later tested when adsorbed to cubosomes (Boge et al., 2017). Results were also similar between free and NP-

bound AMP, but there were slight improvements for conjugated DPK-060 at lower non-bactericidal concentrations, attributed to synergism caused by NP-bacteria interactions. Finally, (Umerska et al., 2017b) tested the activity of two plectasin-derived AMPs adsorbed to lipid nanocapsules. There was synergistic activity for both peptides against *S. aureus*, explained by the antimicrobial compound monolaurin being used as surfactant for the NPs.

Insights on the antimicrobial activity of AMP-NPs could be made from the degradability of PLGA NPs. (Rescignano et al., 2016) evaluated the degradation of PLGA NPs (160 nm) at physiological conditions in PBS. Spherical shape was lost after 14 days and the polymer's M_w decreased across the 21 days tested, but the NPs did not fully degrade. A similar study by (Mohammad & Reineke, 2013) compared the degradation rate of PLGA NPs (200 nm) in vitro and in vivo following intravenous injection in mice. There was a faster reduction of M_w in vivo, which was expected due to the presence of esterases that can accelerate PLGA degradation in physiological medium. Despite its non-fouling effect, PEG has been known to accelerate drug release from PLGA NPs, which suggests faster polymer degradation (Y. Xu et al., 2017). Regardless, these findings indicate NP degradation is insignificant during the maximum 2 hours needed for bactericidal activity and the 24 hours of incubation with bacteria in MIC assays. Therefore, it is safe to assume the AMP can exert action while bound to NPs and the observed antimicrobial effect of AMP-NPs is not due to degradation and AMP release. In eventual in vivo application, the fast antimicrobial effect of the AMP could be complemented by a secondary wound pro-healing effect due to lactate being released through NP degradation.

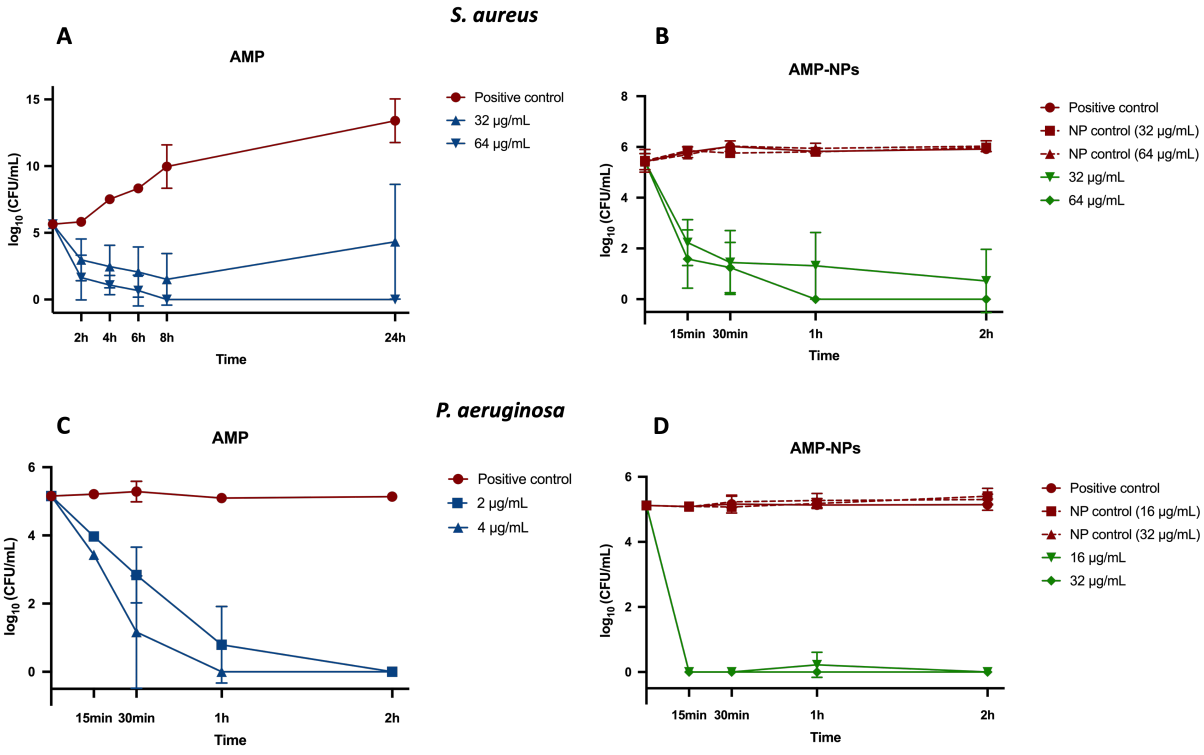

Figure 16 - Results of the time-kill assay of AMP and AMP-NPs. (A) Time-kill curve of AMP against *S. aureus*. (B) Time-kill curve of AMP-NPs against *S. aureus*. (C) Time-kill curve of AMP against *P. aeruginosa*. (D) Time-kill curve of AMP-NPs against *P. aeruginosa*. Values are presented as mean ± SD (n=3).

2.3. Minimum biofilm eradication concentration (MBEC) assay

The antibiofilm activity of AMP and AMP-NPs was assessed against *P. aeruginosa* through the MBEC assay in growth medium. As stated, this species is known to form biofilms in wounds, being correlated with chronicity and decreased treatment efficacy. The same AMP concentrations were tested with and without association to NPs, and a NP control was made with the approximate NP concentration as each AMP-NP sample.

Absorbance reading after crystal violet staining allowed to quantify the biofilm biomass in the pins. All conditions caused a reduction compared to the positive control (biofilm growth check (BGC)), which denotes antibiofilm activity of AMP and AMP-NPs (figure 17). As the positive biofilm control was effectively grown for a total of 3 days, treatment results can be interpreted as the inhibition of biofilm growth for day 3. No complete biofilm eradication was observed up to 128 μg/mL, which is in accordance with the general behavior of AMPs and other antimicrobials being more effective at killing planktonic bacteria than their sessile counterparts. Instead, the percentages of decrease compared to the positive control were calculated. In general, NPs with and without AMP had a more pronounced effect than free AMP. At 128 μg/mL, the AMP and AMP-NPs caused a biofilm inhibition of 32.2 % and 35.6 %, respectively. Interestingly, PLGA-PEG NPs were more effective than AMP-NPs at similar NP concentrations, with 65.5 % reduction of biofilm biomass at 6.52×10^{12} NP/mL. As there was a clear correlation between NP concentration and antibiofilm activity in the NP controls (not present with AMP concentration), the increased effect of AMP-NPs with AMP concentration may have a contribution from the increase of NP concentration. However, a third repetition of this assay must be performed to confirm results.

MSI-78 has been tested against biofilms of DFU-isolated *P. aeruginosa* and led to both biofilm inhibition and eradication at around 100 μg/mL (Gomes et al., 2020), although different conditions were used for biofilm growth. The activity obtained here for MSI-78(4-20) is comparable to that of established AMPs LL-37 and WY-12 at a similar concentration of 50 μM (Pulido et al., 2016). Few AMPs have established antibiofilm activity, especially when it comes to disrupting pre-formed biofilm. It has been posited that the interaction with the negative EPS might prevent AMPs from reaching embedded bacteria (Somma et al., 2020).

The antibiofilm activity of AMPs in combination with NPs has been studied before. Tungsten disulfide QDs combined with peptides KG18 and VR18 led to almost complete removal of *P. aeruginosa* biofilms at 200 μM (Abdul et al., 2019), with QDs having no activity alone but causing over a 2-fold increase of AMP activity. Likewise, AuNPs with covalently immobilized Esc(1-21) via PEG caused a 17-fold increase in efficacy compared to AMP alone (Casciaro et al., 2017). A nanocomposite of AMP, AgNPs and the adhesive compound polydopamine also showed improved activity compared to its individual components (J. Xu et al., 2021). Together, these findings suggest some types of NPs can penetrate biofilms and lead AMPs closer to bacterial cells.

Although not extensively researched, NP interactions with biofilms involve three different mechanisms: transport to the biofilm surface, attachment, and migration through the biofilm matrix. These interactions can be influenced by NP physical properties such as size, shape, surface charge, hydrophobicity and functionalization (Fulaz et al., 2019). Theoretically, positively-charged NPs are more likely to interact with the negative EPS. Such has been reported with QDs – cationic QDs were capable of penetrating *E. coli* biofilms as opposed to neutral or anionic ones (X. Li et al., 2015). However, we found that negative unfunctionalized PLGA-PEG NPs were more effective than positive

AMP-NPs, despite not having any effect in planktonic bacteria. In this case, the close to neutral charge of NPs might allow them to easily migrate through biofilm instead of being bound to its surface due to EPS affinity. Penetration of negative PLGA NPs (100-140 nm) into *P. aeruginosa* biofilms has been documented (Anjum et al., 2019). Besides, the antibiofilm effect of NPs might occur through different mechanisms after penetration. For instance, NPs made of the block copolymer DA95B5 have been shown to disrupt Gram-positive biofilm through debridement of individual bacteria (J. Li et al., 2018).

In future work, a combination of AMP-NPs with PLGA-PEG NPs could be a promising strategy to achieve a balance between antimicrobial and antibiofilm activity, in which NPs initially degrade the biofilm matrix and AMP-NPs kill the remaining planktonic bacteria.

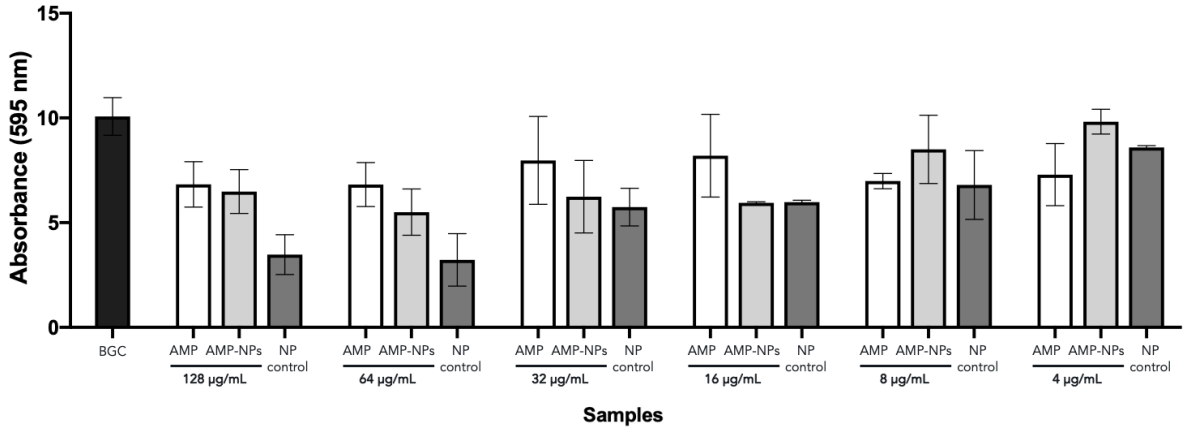

Figure 17 - Results of the MBEC assay on AMP and AMP-NPs. Values are presented as mean ± SD (n=2). Percentages of biofilm reduction at the highest concentration tested were 32.2 % for AMP, 35.6 % for AMP-NPs, and 65.5 % for PLGA-PEG NPs. In these conditions, a concentration-dependent effect is evident for AMP-NPs and PLGA-PEG NPs but not for AMP.

Conclusions and future perspectives

The main purpose of this work was to contribute to the development of novel antibiotic-free treatments for chronic wound infections. Currently-used treatments either present low efficacy, high toxicity, or contribute to development of drug resistance. Particularly, this work also intended to study how the efficacy of AMPs can be improved through conjugation with NPs in order to increase the likelihood of success in the in vivo and clinical environment.

For that, MSI-78(4-20) was chosen, a previously developed AMP which showed equivalent activity and improved selectivity compared to its parent peptide MSI-78. PLGA-PEG NPs were produced by nanoprecipitation and cysteine-modified AMP (MSI-78(4-20)-Ahx-Cys) was immobilized on the NP surface through maleimide-thiol chemistry. Combining AMPs with NPs can potentially lead to increased AMP stability and decreased toxicity. As opposed to loading, surface immobilization can maintain the electrostatic attraction of AMPs to bacterial cells and the fast activity of these molecules due to the lack of dependence on release kinetics.

Except for the adsorption control (AMPads), all NP samples had around 100 nm of diameter and low polydispersity. Surface charge was negative for PLGA-PEG NPs and positive for Mal-AMP samples, with charge being proportional to the ratio of PLGA-PEG-Mal in NPs and suggesting increasing amounts of immobilized AMP. The spherical morphology and size homogeneity of NPs was also confirmed through TEM. The characteristic bands of PLGA-PEG and amino acids were detected in FTIR spectroscopy, and a decrease of the Mal peak detected by NMR spectroscopy confirmed covalent binding of the AMP to NPs. AMP quantification confirmed that 40%Mal-AMP had the highest AMP concentration, highlighting the efficiency of the maleimide-thiol reaction. The inconsistent size and AMP concentration in AMPads denotes that covalent immobilization is a better conjugation strategy overall. At last, NP stability was evaluated in storage at 4 ºC and -80 ºC, with 40%Mal-AMP having considerable aggregation at 4 ºC and a decrease in surface charge taking place in both conditions. Although freezing appears to be the better storage condition, there was still AMP or NP degradation.

The antimicrobial activity of AMP-NPs was assessed against the planktonic pathogens *S. aureus* and *P. aeruginosa* in growth medium. Both AMP and AMP-NPs were more effective against *P. aeruginosa*, which is probably a result of the Gram-negative envelope being more susceptible to AMP disruption, together with the lower electrophoretic mobility of this strain. After AMP immobilization, MIC and MBC values were maintained for *S. aureus* but increased for *P. aeruginosa*, which could be due to a weaker interaction of NP-bound AMP with the outer membrane. Antimicrobial activity was also evaluated in SWF which resembles the composition of the in vivo wound environment. MIC and MBC values against *S. aureus* were the same for AMP-NPs and actually decreased for AMP. On the other hand, there was a general loss of activity against *P. aeruginosa*. This differential effect, which causes a reversal of the trend observed in growth medium, could be explained by AMP affinity in SWF being highest for Gram-positive components (peptidoglycan and TAs), followed by serum components,

and finally lowest for Gram-negative components (outer membrane lipids and LPS). In the future, a detailed study of the affinity of MSI-78(4-20) to bacterial components could be carried out to confirm this theory. Insights could also be taken from studying AMP-NP killing kinetics and antibiofilm activity in SWF. The degradation kinetics of PLGA-PEG NPs should be studied to confirm that NP degradation did not impact antimicrobial activity. Additionally, modifications of AMP or NP structure should be considered to improve activity against Gram-negative pathogens in physiological media. Eventual in vivo assays would allow to study the formulation's antibacterial effectiveness in a relevant model as well as assess if the release of lactate following NP degradation could further improve wound healing.

The killing kinetics of AMP and AMP-NPs were also studied, which revealed a faster activity against *P. aeruginosa* than *S. aureus*. These findings strengthen the theory that the Gram-positive cell wall prevents AMP access to the lipid bilayers with a consequent decrease in effectiveness. Surprisingly, AMP-NPs had a considerably improved killing profile when compared to AMP, which highlights the advantages of immobilization and makes development of drug resistance less likely. Finally, the antibiofilm activity of the conjugate was studied against biofilm-forming *P. aeruginosa*, with AMP-NPs revealing higher biofilm inhibition than AMP. Interestingly, PLGA-PEG NPs had the most pronounced effect, which could be owed to their close to neutral charge allowing penetration through the biofilm matrix. Combining AMP-NPs with PLGA-PEG NPs could be a future prospect to achieve ideal activity against planktonic and sessile bacteria.

Overall, this AMP-NP formulation remains a promising candidate to develop effective antibacterial treatments for chronic wound infections, especially considering the failure rates of conventional antimicrobials and the urgent need for antibiotic-free alternatives.

References

Abdul, S., Ghorai, A., Ilyas, H., Mroue, K. H., Narayanan, G., Sarkare, A., Rayf, S. K., Biswase, K., Berad, A. K., Malmsteng, M., Midyab, A., & Bhuniaa, A. (2019). Application of tungsten disulfide quantum dot-conjugated antimicrobial peptides in bioimaging and antimicrobial therapy. *Colloids and Surfaces B: Biointerfaces*, *176*(2018), 360–370. https://doi.org/10.1016/j.colsurfb.2019.01.020

Almaaytah, A., Mohammed, G. K., Abualhaijaa, A., & Al-Balas, Q. (2017). Development of novel ultrashort antimicrobial peptide nanoparticles with potent antimicrobial and antibiofilm activities against multidrug-resistant bacteria. *Drug Design, Development and Therapy*, *11*, 3159–3170. https://doi.org/10.2147/DDDT.S147450

Andersson, D. I., Hughes, D., & Kubicek-Sutherland, J. Z. (2016). Mechanisms and consequences of bacterial resistance to antimicrobial peptides. *Drug Resistance Updates*, *26*, 43–57. https://doi.org/10.1016/j.drup.2016.04.002

Anjum, A., Chung, P. Y., & Ng, S. F. (2019). PLGA/xylitol nanoparticles enhance antibiofilm activity: Via penetration into biofilm extracellular polymeric substances. *RSC Advances*, *9*(25), 14198–14208. https://doi.org/10.1039/c9ra00125e

Antimicrobial peptides - Wikipedia. (n.d.). Retrieved September 14, 2021, from https://en.wikipedia.org/wiki/Antimicrobial_peptides#Therapeutic_research_and_use

Barrero-Guevara, L. A., Bolaños, N., Parra, M., González, J. M., Groot, H., & Muñoz-Camargo, C. (2019). New peptides with immunomodulatory activity in macrophages and antibacterial activity against multiresistant Staphylococcus aureus. *BioRxiv*. https://doi.org/10.1101/838201

Bayer, M. E., & Sloyer, J. L. (1990). The electrophoretic mobility of Gram-negative and Gram-positive bacteria: an electrokinetic analysis. *Journal of General Microbiology*, *136*(5), 867–874. https://doi.org/10.1099/00221287-136-5-867

Bessa, L. J., Fazii, P., Di Giulio, M., & Cellini, L. (2015). Bacterial isolates from infected wounds and their antibiotic susceptibility pattern: Some remarks about wound infection. *International Wound Journal*, *12*(1), 47–52. https://doi.org/10.1111/iwj.12049

Björn, C., Håkansson, J., Myhrman, E., Sjöstrand, V., Haug, T., Lindgren, K., Blencke, H.-M., Stensvåg, K., & Mahlapuu, M. (2012). Anti-infectious and anti-inflammatory effects of peptide fragments sequentially derived from the antimicrobial peptide centrocin 1 isolated from the green sea urchin, Strongylocentrotus droebachiensis. *AMB Express*, *2*(1), 67. https://doi.org/10.1186/2191-0855-2-67

Boge, A. L., Umerska, A., Matougui, N., Bysell, H., Ringstad, L., & Davoudi, M. (2017). Cubosomes post-loaded with antimicrobial peptides: characterization, bactericidal effect and proteolytic

stability. *International Journal of Pharmaceutics*, *4*. https://doi.org/10.1016/j.ijpharm.2017.04.082

Boge, L., Bysell, H., Ringstad, L., Wennman, D., Umerska, A., Cassisa, V., Eriksson, J., Joly-Guillou, M. L., Edwards, K., & Andersson, M. (2016). Lipid-Based Liquid Crystals As Carriers for Antimicrobial Peptides: Phase Behavior and Antimicrobial Effect. *Langmuir*, *32*(17), 4217–4228. https://doi.org/10.1021/acs.langmuir.6b00338

Boge, L., Hallstensson, K., Ringstad, L., Johansson, J., Davoudi, M., Larsson, P. T., Mahlapuu, M., & Andersson, M. (2018). Cubosomes for topical delivery of the antimicrobial peptide LL-37. *European Journal of Pharmaceutics and Biopharmaceutics*, *11*. https://doi.org/10.1016/j.ejpb.2018.11.009

Braun, K., Pochert, A., Gerber, M., Raber, H. F., & Lindén, M. (2017). Influence of mesopore size and peptide aggregation on the adsorption and release of a model antimicrobial peptide onto/from mesoporous silica nanoparticles in vitro. *Molecular Systems Design & Engineering*. https://doi.org/10.1039/C7ME00059F

Braun, K., Pochert, A., Lindén, M., Davoudi, M., Schmidtchen, A., Nordström, R., & Malmsten, M. (2016). Membrane interactions of mesoporous silica nanoparticles as carriers of antimicrobial peptides. *Journal of Colloid and Interface Science*, *475*, 161–170. https://doi.org/10.1016/j.jcis.2016.05.002

Carpenter, C. F., & Chambers, H. F. (2004). Daptomycin: Another novel agent for treating infections due to drug-resistant gram-positive pathogens. *Clinical Infectious Diseases*, *38*(7), 994–1000. https://doi.org/10.1086/383472

Casciaro, B., Moros, M., Rivera-Fernández, S., Bellelli, A., de la Fuente, J. M., & Mangoni, M. L. (2017). Gold-nanoparticles coated with the antimicrobial peptide esculentin-1a(1-21)NH2 as a reliable strategy for antipseudomonal drugs. *Acta Biomaterialia*, *47*, 170–181. https://doi.org/10.1016/j.actbio.2016.09.041

Cascini, S., Agabiti, N., Davoli, M., Uccioli, L., Meloni, M., Giurato, L., Marino, C., & Bargagli, A. M. (2020). Survival and factors predicting mortality after major and minor lower-extremity amputations among patients with diabetes: A population-based study using health information systems. *BMJ Open Diabetes Research and Care*, *8*(1), 1–8. https://doi.org/10.1136/bmjdrc-2020-001355

Chemical Book. (n.d.). *Maleimide(541-59-3) 1H NMR*. Retrieved July 24, 2021, from https://www.chemicalbook.com/SpectrumEN_541-59-3_1HNMR.htm

Chen, C. H., & Lu, T. K. (2020). Development and challenges of antimicrobial peptides for therapeutic applications. *Antibiotics*, *9*(1). https://doi.org/10.3390/antibiotics9010024

Chen, W. Y., Chang, H. Y., Lu, J. K., Huang, Y. C., Harroun, S. G., Tseng, Y. T., Li, Y. J., Huang, C. C., & Chang, H. T. (2015). Self-Assembly of Antimicrobial Peptides on Gold Nanodots: Against Multidrug-Resistant Bacteria and Wound-Healing Application. *Advanced Functional Materials*, *25*(46), 7189–7199. https://doi.org/10.1002/adfm.201503248

Cheng-Foh, L., & Chee-Mun, F. (2017). Intracellular Targeting Mechanisms by Antimicrobial Peptides. *Antimicrobial Agents and Chemotherapy*, *61*(4), 1–16. https://aac.asm.org/content/61/4/e02340-16

Chereddy, K. K., Her, C. H., Comune, M., Moia, C., Lopes, A., Porporato, P. E., Vanacker, J., Lam, M. C., Steinstraesser, L., Sonveaux, P., Zhu, H., Ferreira, L. S., Vandermeulen, G., & Préat, V. (2014). PLGA nanoparticles loaded with host defense peptide LL37 promote wound healing. *Journal of Controlled Release*, *194*, 138–147. https://doi.org/10.1016/j.jconrel.2014.08.016

Chereddy, K. K., Vandermeulen, G., & Préat, V. (2016). PLGA based drug delivery systems:

Promising carriers for wound healing activity. *Wound Repair and Regeneration*, *24*(2), 223–236. https://doi.org/10.1111/wrr.12404

Christaki, E., Marcou, M., & Tofarides, A. (2020). Antimicrobial Resistance in Bacteria: Mechanisms, Evolution, and Persistence. *Journal of Molecular Evolution*, *88*(1), 26–40. https://doi.org/10.1007/s00239-019-09914-3

Cruz, J., Flórez, J., Torres, R., Urquiza, M., Gutiérrez, J. A., Guzmán, F., & Ortiz, C. C. (2017). Antimicrobial activity of a new synthetic peptide loaded in polylactic acid or poly(lactic-co-glycolic) acid nanoparticles against Pseudomonas aeruginosa, Escherichia coli O157:H7 and methicillin resistant Staphylococcus aureus (MRSA). *Nanotechnology*, *28*(13). https://doi.org/10.1088/1361-6528/aa5f63

Danhier, F., Ansorena, E., Silva, J. M., Coco, R., Le Breton, A., & Préat, V. (2012). PLGA-based nanoparticles: An overview of biomedical applications. *Journal of Controlled Release*, *161*(2), 505–522. https://doi.org/10.1016/j.jconrel.2012.01.043

de Kraker, M. E. A., Stewardson, A. J., & Harbarth, S. (2016). Will 10 Million People Die a Year due to Antimicrobial Resistance by 2050? *PLoS Medicine*, *13*(11), 1–6. https://doi.org/10.1371/journal.pmed.1002184

Demidova-Rice, T. N. T. N., Hamblin, M. R. M. R., & Herman, I. . I. M. (2012). Acute and Impaired Wound Healing: Pathophysiology and Current Methods for Drug Delivery, Part 1: Normal and Chronic Wounds: Biology, Causes, and Approaches to Care. *Advances in Skin and Wound Care*, *25*(8), 304–314. https://doi.org/10.1097/01.ASW.0000416006.55218.d0.Acute

Deslouches, B., & Peter Di, Y. (2017). Antimicrobial peptides with selective antitumor mechanisms: Prospect for anticancer applications. *Oncotarget*, *8*(28), 46635–46651. https://doi.org/10.18632/oncotarget.16743

Deygen, I. M., & Kudryashova, E. V. (2016). New versatile approach for analysis of PEG content in conjugates and complexes with biomacromolecules based on FTIR spectroscopy. *Colloids and Surfaces B: Biointerfaces*, *141*, 36–43. https://doi.org/10.1016/j.colsurfb.2016.01.030

Di Somma, A., Moretta, A., Canè, C., Cirillo, A., & Duilio, A. (2020). Antimicrobial and antibiofilm peptides. *Biomolecules*, *10*(4), 1–15. https://doi.org/10.3390/biom10040652

ECDC. (2020). *Antimicrobial resistance in the EU/EEA (EARS-Net) - AER for 2019*. https://www.ecdc.europa.eu/en/publications-data/surveillance-antimicrobial-resistance-europe-2019

Edwards, R., & Harding, K. G. (2004). Bacteria and wound healing. *Current Opinion in Infectious Diseases*, *17*(2), 91–96. https://doi.org/10.1097/00001432-200404000-00004

Ernst, C. M., Staubitz, P., Mishra, N. N., Yang, S. J., Hornig, G., Kalbacher, H., Bayer, A. S., Kraus, D., & Peschel, A. (2009). The bacterial defensin resistance protein MprF consists of separable domains for lipid lysinylation and antimicrobial peptide repulsion. *PLoS Pathogens*, *5*(11), 1–9. https://doi.org/10.1371/journal.ppat.1000660

Fernandez, J., Acosta, G., Pulido, D., Malý, M., Copa-Patiño, J. L., Soliveri, J., Royo, M., Gómez, R., Albericio, F., Ortega, P., & De La Mata, F. J. (2019). Carbosilane Dendron-Peptide Nanoconjugates as Antimicrobial Agents. *Molecular Pharmaceutics*, *16*(6), 2661–2674. https://doi.org/10.1021/acs.molpharmaceut.9b00222

Finkelstein, E. A., Khavjou, O. A., Thompson, H., Trogdon, J. G., Pan, L., Sherry, B., & Dietz, W. (2012). Obesity and severe obesity forecasts through 2030. *American Journal of Preventive Medicine*, *42*(6), 563–570. https://doi.org/10.1016/j.amepre.2011.10.026

Fosgerau, K., & Hoffmann, T. (2015). Peptide therapeutics: Current status and future directions. *Drug Discovery Today*, *20*(1), 122–128. https://doi.org/10.1016/j.drudis.2014.10.003

Fulaz, S., Vitale, S., Quinn, L., & Casey, E. (2019). Nanoparticle–Biofilm Interactions: The Role of the EPS Matrix. *Trends in Microbiology*, *27*(11), 915–926. https://doi.org/10.1016/j.tim.2019.07.004

Galdiero, E., Siciliano, A., Maselli, V., Gesuele, R., Guida, M., Fulgione, D., Galdiero, S., Lombardi, L., & Falanga, A. (2016). An integrated study on antimicrobial activity and ecotoxicity of quantum dots and quantum dots coated with the antimicrobial peptide indolicidin. *International Journal of Nanomedicine*, *11*, 4199–4211.

Gao, J., Na, H., Zhong, R., Yuan, M., Guo, J., Zhao, L., Wang, Y., Wang, L., & Zhang, F. (2019). One step synthesis of antimicrobial peptide protected silver nanoparticles: the core-shell mutual enhancement of antibacterial activity. *Colloids and Surfaces B: Biointerfaces*, *110704*(November). https://doi.org/10.1016/j.colsurfb.2019.110704

Gao, W., Thamphiwatana, S., Angsantikul, P., & Zhang, L. (2014). Nanoparticle approaches against bacterial infections. In *Wiley Interdisciplinary Reviews: Nanomedicine and Nanobiotechnology*. https://doi.org/10.1002/wnan.1282

Garcia-orue, I., Gainza, G., Girbau, C., Alonso, R., Javier, J., Luis, J., Igartua, M., & Maria, R. (2016). LL37 loaded nanostructured lipid carriers (NLC): A new strategy for the topical treatment of chronic wounds. *European Journal of Pharmaceutics and Biopharmaceutics*. https://doi.org/10.1016/j.ejpb.2016.04.006

Ge, Y., MacDonald, D. L., Holroyd, K. J., Thornsberry, C., Wexler, H., & Zasloff, M. (1999). In vitro antibacterial properties of pexiganan, an analog of magainin. *Antimicrobial Agents and Chemotherapy*, *43*(4), 782–788. https://doi.org/10.1128/aac.43.4.782

Gilding, D. K., & Reed, A. M. (1979). Biodegradable polymers for use in surgery-polyglycolic/poly(lactic acid) homo- and copolymers: 1. *Polymer*, *20*(12), 1459–1464. https://doi.org/10.1016/0032-3861(79)90009-0

Gjødsbøl, K., Christensen, J. J., Karlsmark, T., Jørgensen, B., Klein, B. M., & Krogfelt, K. A. (2006). Multiple bacterial species reside in chronic wounds: A longitudinal study. *International Wound Journal*, *3*(3), 225–231. https://doi.org/10.1111/j.1742-481X.2006.00159.x

Gläser, R., Becker, K., Von Eiff, C., Meyer-Hoffert, U., & Harder, J. (2014). Decreased susceptibility of staphylococcus aureus small-colony variants toward human antimicrobial peptides. *Journal of Investigative Dermatology*, *134*(9), 2347–2350. https://doi.org/10.1038/jid.2014.176

Gomes, D., Santos, R., Soares, R. S., Reis, S., Carvalho, S., Rego, P., Peleteiro, M. C., Tavares, L., & Oliveira, M. (2020). Pexiganan in combination with nisin to control polymicrobial diabetic foot infections. *Antibiotics*, *9*(3), 1–15. https://doi.org/10.3390/antibiotics9030128

Gottler, L. M., & Ramamoorthy, A. (2009). Structure, Membrane Orientation, Mechanism, and Function of Pexiganan – A Highly Potent Antimicrobial Peptide Designed From Magainin. *Biochimica et Biophysica Acta*, *1788*(8), 1680–1686. https://doi.org/10.1038/jid.2014.371

Gounani, Z., Asadollahi, M. A., Meyer, R. L., & Arpanaei, A. (2018). Loading of polymyxin B onto anionic mesoporous silica nanoparticles retains antibacterial activity and enhances biocompatibility. *International Journal of Pharmaceutics*, *537*(1–2), 148–161. https://doi.org/10.1016/j.ijpharm.2017.12.039

Gram Staining | BioNinja. (n.d.). Retrieved July 26, 2021, from https://ib.bioninja.com.au/options/untitled/b1-microbiology-organisms/gram-staining.html

Grönberg, A., Mahlapuu, M., Ståhle, M., Whately-Smith, C., & Rollman, O. (2014). Treatment with LL-37 is safe and effective in enhancing healing of hard-to-heal venous leg ulcers: a randomized, placebo-controlled clinical trial. *Wound Repair and Regeneration*, *22*(5), 613–621. https://doi.org/10.1111/wrr.12211

Groo, A., Matougui, N., Umerska, A., & Saulnier, P. (2018). Reverse micelle-lipid nanocapsules : a novel strategy for drug delivery of the plectasin derivate AP138 antimicrobial peptide. *International Journal of Nanomedicine*, *13*, 7565–7574.

Guo, S., & DiPietro, L. A. (2010). Factors affecting wound healing. *Journal of Dental Research*, *89*(3), 219–229. https://doi.org/10.1177/0022034509359125

Habets, M. G. J. L., & Brockhurst, M. A. (2012). Therapeutic antimicrobial peptides may compromise natural immunity. *Biology Letters*, *8*(3), 416–418. https://doi.org/10.1098/rsbl.2011.1203

Hallett, J. W., Wolkowicz, M. I., & Leopold, I. H. (1956). Ophthalmic use of neosporin. *American Journal of Ophthalmology*, *41*(5), 850–853. https://doi.org/10.1016/0002-9394(56)91781-0

Hassan, M., Kjos, M., Nes, I. F., Diep, D. B., & Lotfipour, F. (2012). Natural antimicrobial peptides from bacteria: Characteristics and potential applications to fight against antibiotic resistance. *Journal of Applied Microbiology*, *113*(4), 723–736. https://doi.org/10.1111/j.1365-2672.2012.05338.x

Held, P. B. I. (2006). Fluorimetric Quantitation of Protein using the Reactive Compound Fluorescamine. *Nature Methods| Application Notes*, *1*(22), 1–5. https://doi.org/10.1038/an1794

Henderson, B., Nair, S., Pallas, J., & Williams, M. A. (2011). Fibronectin: A multidomain host adhesin targeted by bacterial fibronectin-binding proteins. *FEMS Microbiology Reviews*, *35*(1), 147–200. https://doi.org/10.1111/j.1574-6976.2010.00243.x

Hermans, P. E., & Wilhelm, M. P. (1987). Vancomycin. *Mayo Clinic Proceedings*, *62*(10), 901–905. https://doi.org/10.1016/S0025-6196(12)65046-0

Horcajada, J. P., Montero, M., Oliver, A., Sorlí, L., Luque, S., Gómez-Zorrilla, S., Benito, N., & Grau, S. (2019). Epidemiology and treatment of multidrug-resistant and extensively drug-resistant Pseudomonas aeruginosa infections. *Clinical Microbiology Reviews*, *32*(4), 1–52. https://doi.org/10.1128/CMR.00031-19

Jalaei, J., Layeghi-Ghalehsoukhteh, S., Hosseini, A., & Fazeli, M. (2018). Antibacterial effects of gold nanoparticles functionalized with the extracted peptide from Vespa orientalis wasp venom. *Journal of Peptide Science*, *24*(12), 1–10. https://doi.org/10.1002/psc.3124

James, G. A., Swogger, E., Wolcott, R., Pulcini, E. D., Secor, P., Sestrich, J., Costerton, J. W., & Stewart, P. S. (2008). Biofilms in chronic wounds. *Wound Repair and Regeneration*, *16*(1), 37–44. https://doi.org/10.1111/j.1524-475X.2007.00321.x

Kalashnikova, I., Das, S., & Seal, S. (2015). Nanomaterials for wound healing: Scope and advancement. *Nanomedicine*, *10*(16), 2593–2612. https://doi.org/10.2217/nnm.15.82

Kang, X., Dong, F., Shi, C., Liu, S., Sun, J., Chen, J., Li, H., Xu, H., Lao, X., & Zheng, H. (2019). DRAMP 2.0, an updated data repository of antimicrobial peptides. *Scientific Data*, *6*(1). https://doi.org/10.1038/s41597-019-0154-y

Khansa, I., Schoenbrunner, A. R., Kraft, C. T., & Janis, J. E. (2019). Silver in Wound Care - Friend or Foe?: A Comprehensive Review. *Plastic and Reconstructive Surgery - Global Open*, *7*(8), 1–10. https://doi.org/10.1097/GOX.0000000000002390

Kim, Y., Ho, S. O., Gassman, N. R., Korlann, Y., Landorf, E. V., Collart, F. R., & Weiss, S. (2008). Efficient Site-Specific Labeling of Proteins via Cysteines. *Bioconjugate Chemistry*, *19*(3), 786–791. https://doi.org/10.1021/bc7002499.Efficient

Ko, S. J., Park, E., Asandei, A., Choi, J. Y., Lee, S. C., Seo, C. H., Luchian, T., & Park, Y. (2020). Bee venom-derived antimicrobial peptide melectin has broad-spectrum potency, cell selectivity, and salt-resistant properties. *Scientific Reports*, *10*(1), 1–12.

https://doi.org/10.1038/s41598-020-66995-7

Kong, J., & Yu, S. (2007). Fourier transform infrared spectroscopic analysis of protein secondary structures. *Acta Biochimica et Biophysica Sinica*, *39*(8), 549–559. https://doi.org/10.1111/j.1745-7270.2007.00320.x

Koo, H. B., & Seo, J. (2019). Antimicrobial peptides under clinical investigation. *Peptide Science*, *111*(5). https://doi.org/10.1002/pep2.24122

Kwa, A., Kasiakou, S. K., Tam, V. H., & Falagas, M. E. (2007). Polymyxin B: Similarities to and differences from colistin (polymyxin E). *Expert Review of Anti-Infective Therapy*, *5*(5), 811–821. https://doi.org/10.1586/14787210.5.5.811

Kwon, J. Y., Kim, M. K., Mereuta, L., Seo, C. H., Luchian, T., & Park, Y. (2019). Mechanism of action of antimicrobial peptide P5 truncations against Pseudomonas aeruginosa and Staphylococcus aureus. *AMB Express*, *9*(1). https://doi.org/10.1186/s13568-019-0843-0

Laato, M., Niinikoski, J., Lundberg, C., & Gerdin, B. (1988). Inflammatory reaction and blood flow in experimental wounds inoculated with Staphylococcus aureus. *European Surgical Research*, *20*(1), 33–38. https://doi.org/10.1159/000128738

Lakhundi, S., & Zhang, K. (2018). Methicillin-Resistant Staphylococcus aureus: Molecular Characterization, Evolution, and Epidemiology. *Clinical Microbiology Reviews*, *31*(4), 1–103. https://doi.org/10.1128/CMR.00020-18

Lalloz, A., Bolzinger, M. A., Briançon, S., Faivre, J., Rabanel, J. M., Garcia Ac, A., Hildgen, P., & Banquy, X. (2019). Subtle and unexpected role of PEG in tuning the penetration mechanisms of PLA-based nano-formulations into intact and impaired skin. *International Journal of Pharmaceutics*, *563*(February), 79–90. https://doi.org/10.1016/j.ijpharm.2019.02.039

Lambadi, P. R., Sharma, T. K., Kumar, P., Vasnani, P., Thalluri, S. M., Bisht, N., Pathania, R., & Navani, N. K. (2015). Facile biofunctionalization of silver nanoparticles for enhanced antibacterial properties, endotoxin removal, and biofilm control. *International Journal of Nanomedicine*, *10*, 2155–2171. https://doi.org/10.2147/IJN.S72923

Lee, K., & Yoon, S. S. (2017). Pseudomonas aeruginosa Biofilm, a Programmed Bacterial Life for Fitness. *Journal of Microbiology and Biotechnology*, *27*(6), 1053–1064. https://doi.org/10.4014/jmb.1611.11056

Lerminiaux, N. A., & Cameron, A. D. S. (2019). Horizontal transfer of antibiotic resistance genes in clinical environments. *Canadian Journal of Microbiology*, *65*(1), 34–44. https://doi.org/10.1139/cjm-2018-0275

Li, J., Zhang, K., Ruan, L., Chin, S. F., Wickramasinghe, N., Liu, H., Ravikumar, V., Ren, J., Duan, H., Yang, L., & Chan-Park, M. B. (2018). Block Copolymer Nanoparticles Remove Biofilms of Drug-Resistant Gram-Positive Bacteria by Nanoscale Bacterial Debridement. *Nano Letters*, *18*(7), 4180–4187. https://doi.org/10.1021/acs.nanolett.8b01000

Li, M., Cha, D. J., Lai, Y., Villaruz, A. E., Sturdevant, D. E., & Otto, M. (2007). The antimicrobial peptide-sensing system aps of Staphylococcus aureus. *Molecular Microbiology*, *66*(5), 1136–1147. https://doi.org/10.1111/j.1365-2958.2007.05986.x

Li, X., Yeh, Y. C., Giri, K., Mout, R., Landis, R. F., Prakash, Y. S., & Rotello, V. M. (2015). Control of nanoparticle penetration into biofilms through surface design. *Chemical Communications*, *51*(2), 282–285. https://doi.org/10.1039/c4cc07737g

Lipsky, B. A., Holroyd, K. J., & Zasloff, M. (2008). Topical versus Systemic Antimicrobial Therapy for Treating Mildly Infected Diabetic Foot Ulcers: A Randomized, Controlled, Double-Blinded, Multicenter Trial of Pexiganan Cream. *Clinical Infectious Diseases*, *47*(12), 1537–1545. https://doi.org/10.1086/593185

Llobet, E., Tomás, J. M., & Bengoechea, J. A. (2008). Capsule polysaccharide is a bacterial decoy for antimicrobial peptides. *Microbiology*, *154*(12), 3877–3886. https://doi.org/10.1099/mic.0.2008/022301-0

Mahlapuu, M., Håkansson, J., Ringstad, L., & Björn, C. (2016). Antimicrobial peptides: An emerging category of therapeutic agents. *Frontiers in Cellular and Infection Microbiology*, *6*(December), 1–12. https://doi.org/10.3389/fcimb.2016.00194

Malanovic, N., & Lohner, K. (2016). Gram-positive bacterial cell envelopes: The impact on the activity of antimicrobial peptides. *Biochimica et Biophysica Acta - Biomembranes*, *1858*(5), 936–946. https://doi.org/10.1016/j.bbamem.2015.11.004

Maleki, H., Rai, A., Pinto, S., Evangelista, M., Cardoso, R. M. S., Paulo, C., Carvalheiro, T., Paiva, A., Imani, M., Simchi, A., Durães, L., Portugal, A., & Ferreira, L. (2016). High Antimicrobial Activity and Low Human Cell Cytotoxicity of Core-Shell Magnetic Nanoparticles Functionalized with an Antimicrobial Peptide. *ACS Applied Materials and Interfaces*, *8*(18), 11366–11378. https://doi.org/10.1021/acsami.6b03355

Malone, M., Bjarnsholt, T., McBain, A. J., James, G. A., Stoodley, P., Leaper, D., Tachi, M., Schultz, G., Swanson, T., & Wolcott, R. D. (2017). The prevalence of biofilms in chronic wounds: A systematic review and meta-analysis of published data. *Journal of Wound Care*, *26*(1), 20–25. https://doi.org/10.12968/jowc.2017.26.1.20

Manikkath, J., Sumathy, T., Manikkath, A., & Mutalik, S. (2018). Delving Deeper into Dermal and Transdermal Drug Delivery: Factors and Mechanisms Associated with Nanocarrier-mediated Strategies. *Current Pharmaceutical Design*, *24*(27), 3210–3222. https://doi.org/10.2174/1381612824666180924122640

Manniello, J. M., Heymann, H., & Adair, F. W. (1978). Resistance of spheroplasts and whole cells of Pseudomonas cepacia to polymyxin B. *Antimicrobial Agents and Chemotherapy*, *14*(3), 500–504. https://doi.org/10.1128/AAC.14.3.500

Manosroi, A., Kongkaneramit, L., & Manosroi, J. (2004). Stability and transdermal absorption of topical amphotericin B liposome formulations. *International Journal of Pharmaceutics*, *270*(1–2), 279–286. https://doi.org/10.1016/j.ijpharm.2003.10.031

Mazumdar, A., Haddad, Y., Milosavljevic, V., Michalkova, H., Guran, R., Bhowmick, S., & Moulick, A. (2020). Peptide-Carbon Quantum Dots Conjugate, Derived from Human Retinoic Acid Receptor Responder Protein 2, against Antibiotic-Resistant Gram Positive and Gram Negative Pathogenic Bacteria. *Nanomaterials*, *10*(325).

McLaughlin, S., Ahumada, M., Franco, W., Mah, T. F., Seymour, R., Suuronen, E. J., & Alarcon, E. I. (2016). Sprayable peptide-modified silver nanoparticles as a barrier against bacterial colonization. *Nanoscale*, *8*(46), 19200–19203. https://doi.org/10.1039/c6nr07976h

Meikle, T. G., Zabara, A., Waddington, L. J., Separovic, F., Drummond, C. J., & Conn, C. E. (2017). Incorporation of antimicrobial peptides in nanostructured lipid membrane mimetic bilayer cubosomes. *Colloids and Surfaces B: Biointerfaces*, *152*, 143–151. https://doi.org/10.1016/j.colsurfb.2017.01.004

Mir, M., Ahmed, N., & Rehman, A. ur. (2017). Recent applications of PLGA based nanostructures in drug delivery. *Colloids and Surfaces B: Biointerfaces*, *159*, 217–231. https://doi.org/10.1016/j.colsurfb.2017.07.038

Mohammad, A. K., & Reineke, J. J. (2013). Quantitative detection of PLGA nanoparticle degradation in tissues following intravenous administration. *Molecular Pharmaceutics*, *10*(6), 2183–2189. https://doi.org/10.1021/mp300559v

Monteiro, C., Fernandes, H., Oliveira, D., Vale, N., Barbosa, M., Gomes, P., & Martins, M. C. L.

(2020). AMP–Chitosan Coating with Bactericidal Activity in the Presence of Human Plasma Proteins. *Molecules*, *25*(3046).

Monteiro, C., Pinheiro, M., Fernandes, M., Maia, S., Seabra, C. L., Ferreira-Da-Silva, F., Reis, S., Gomes, P., & Martins, M. C. L. (2015). A 17-mer Membrane-Active MSI-78 Derivative with Improved Selectivity toward Bacterial Cells. *Molecular Pharmaceutics*, *12*(8), 2904–2911. https://doi.org/10.1021/acs.molpharmaceut.5b00113

Moore, R., Bates, N. C., & Hancock, R. E. W. (1986). Interaction of polycationic antibiotics with Pseudomonas aeruginosa Lipopolysaccharide and lipid A studied by using dansyl-polymyxin. *Antimicrobial Agents and Chemotherapy*, *29*(3), 496–500. https://doi.org/10.1128/AAC.29.3.496

Myhrman, E., Håkansson, J., Lindgren, K., Björn, C., Sjöstrand, V., & Mahlapuu, M. (2013). The novel antimicrobial peptide PXL150 in the local treatment of skin and soft tissue infections. *Applied Microbiology and Biotechnology*, *97*(7), 3085–3096. https://doi.org/10.1007/s00253-012-4439-8

Nilsson, A. C., Janson, H., Wold, H., Fugelli, A., Andersson, K., Håkangård, C., Olsson, P., & Olsen, W. M. (2015). Ltx-109 is a novel agent for nasal decolonization of methicillin-resistant and -sensitive Staphylococcus aureus. *Antimicrobial Agents and Chemotherapy*, *59*(1), 145–151. https://doi.org/10.1128/AAC.03513-14

NNIS. (2003). National Nosocomial Infections Surveillance (NNIS) System Report, data summary from January 1992 through June 2003, issued August 2003. *American Journal of Infection Control*, *31*(8), 481–498. https://doi.org/10.1016/j.ajic.2003.09.002

Nussbaum, S. R., Carter, M. J., Fife, C. E., DaVanzo, J., Haught, R., Nusgart, M., & Cartwright, D. (2018). An Economic Evaluation of the Impact, Cost, and Medicare Policy Implications of Chronic Nonhealing Wounds. *Value in Health*, *21*(1), 27–32. https://doi.org/10.1016/j.jval.2017.07.007

Otagiri, M., Giam Chuang, V. T., Immunobiology, Murphy, K., & Weaver, C. (2017). Janeway's 9th Edition. In *America*. https://doi.org/10.1007/978-981-10-2116-9

Ovington, L. (2003). Bacterial toxins and wound healing. *Ostomy Wound Management*, *49*(7A Suppl.), 8–12.

Pal, I., Bhattacharyya, D., Kar, R. K., Zarena, D., Bhunia, A., & Atreya, H. S. (2019). A Peptide-Nanoparticle System with Improved Efficacy against Multidrug Resistant Bacteria. *Scientific Reports*, *9*(1), 1–12. https://doi.org/10.1038/s41598-019-41005-7

Park, Y., Park, S. C., Park, H. K., Shin, S. Y., Kim, Y., & Hahm, K. S. (2007). Structure-activity relationship of HP (2-20) analog peptide: Enhanced antimicrobial activity by N-terminal random coil region deletion. *Biopolymers - Peptide Science Section*, *88*(2), 199–207. https://doi.org/10.1002/bip.20679

Patocka, J., Nepovimova, E., Klimova, B., & Kuca, K. (2018). Antimicrobial Peptides: Amphibian Host Defense Peptides. *Current Medicinal Chemistry*, *26*(32), 5924–5946. https://doi.org/10.2174/0929867325666180713125314

Patra, J. K., Das, G., Fraceto, L. F., Campos, E. V. R., Rodriguez-Torres, M. D. P., Acosta-Torres, L. S., Diaz-Torres, L. A., Grillo, R., Swamy, M. K., Sharma, S., Habtemariam, S., & Shin, H. S. (2018). Nano based drug delivery systems: Recent developments and future prospects. *Journal of Nanobiotechnology*, *16*(1), 1–33. https://doi.org/10.1186/s12951-018-0392-8

Pelgrift, R. Y., & Friedman, A. J. (2013). Nanotechnology as a therapeutic tool to combat microbial resistance. *Advanced Drug Delivery Reviews*, *65*(13–14), 1803–1815. https://doi.org/10.1016/j.addr.2013.07.011

Perfectus Biomed Group. (2017). *CBE Regulatory Meeting: Anti-Biofilm Technologies: Pathways to Product Development*. https://perfectusbiomed.com/cbe-meeting-anti-biofilm-technologies/

Piktel, E., Wnorowska, U., Cieśluk, M., Deptula, P., Pogoda, K., Misztalewska-Turkowicz, I., Paprocka, P., Niemirowicz-Laskowska, K., Wilczewska, A. Z., Janmey, P. A., & Bucki, R. (2019). Inhibition of inflammatory response in human keratinocytes by magnetic nanoparticles functionalized with PBP10 peptide derived from the PIP2-binding site of human plasma gelsolin. *Journal of Nanobiotechnology*, *17*(1), 1–19. https://doi.org/10.1186/s12951-019-0455-5

Piras, A. M., Sandreschi, S., Maisetta, G., Esin, S., Batoni, G., & Chiellini, F. (2015). Chitosan nanoparticles for the linear release of model cationic peptide. *Pharmaceutical Research*, *32*(7), 2259–2265. https://doi.org/10.1007/s11095-014-1615-9

Pires, J., Siriwardena, T. N., Stach, M., Tinguely, R., Kasraian, S., Luzzaro, F., Leib, S. L., Darbre, T., Reymond, J. L., & Endimiani, A. (2015). In Vitro activity of the novel antimicrobial peptide dendrimer G3KL against multidrug-resistant Acinetobacter baumannii and Pseudomonas aeruginosa. *Antimicrobial Agents and Chemotherapy*, *59*(12), 7915–7918. https://doi.org/10.1128/AAC.01853-15

Pirtskhalava, M., Amstrong, A. A., Grigolava, M., Chubinidze, M., Alimbarashvili, E., Vishnepolsky, B., Gabrielian, A., Rosenthal, A., Hurt, D. E., & Tartakovsky, M. (2021). DBAASP v3: Database of antimicrobial/cytotoxic activity and structure of peptides as a resource for development of new therapeutics. *Nucleic Acids Research*, *49*(D1), D288–D297. https://doi.org/10.1093/nar/gkaa991

Podolsky, S. H. (2018). The evolving response to antibiotic resistance (1945–2018). *Palgrave Communications*, *4*(1). https://doi.org/10.1057/s41599-018-0181-x

Porcelli, F., Buck-Koehntop, B. A., Thennarasu, S., Ramamoorthy, A., & Veglia, G. (2006). Structures of the dimeric and monomeric variants of magainin antimicrobial peptides (MSI-78 and MSI-594) in micelles and bilayers, determined by NMR spectroscopy. *Biochemistry*, *45*(18), 5793–5799. https://doi.org/10.1021/bi0601813

Porporato, P. E., Payen, V. L., De Saedeleer, C. J., Préat, V., Thissen, J. P., Feron, O., & Sonveaux, P. (2012). Lactate stimulates angiogenesis and accelerates the healing of superficial and ischemic wounds in mice. *Angiogenesis*, *15*(4), 581–592. https://doi.org/10.1007/s10456-012-9282-0

Power, C., Wang, J. H., Sookhai, S., Street, J. T., & Redmond, H. P. (2001). Bacterial wall products induce downregulation of vascular endothelial growth factor receptors on endothelial cells via a CD14-dependent mechanism: Implications for surgical wound healing. *Journal of Surgical Research*, *101*(2), 138–145. https://doi.org/10.1006/jsre.2001.6270

Powers, J. G., Higham, C., Broussard, K., & Phillips, T. J. (2016). Wound healing and treating wounds Chronic wound care and management. *Journal of the American Academy of Dermatology*, *74*(4), 607–625. https://doi.org/10.1016/j.jaad.2015.08.070

Price, B. L., Lovering, A. M., Bowling, F. L., & Dobson, C. B. (2016). Development of a novel collagen wound model to simulate the activity and distribution of antimicrobials in soft tissue during diabetic foot infection. *Antimicrobial Agents and Chemotherapy*, *60*(11), 6880–6889. https://doi.org/10.1128/AAC.01064-16

Pulido, D., Prats-Ejarque, G., Villalba, C., Albacar, M., González-López, J. J., Torrent, M., Moussaoui, M., & Boix, E. (2016). A novel RNase 3/ECP peptide for Pseudomonas aeruginosa biofilm eradication that combines antimicrobial, lipopolysaccharide binding, and cell-agglutinating activities. *Antimicrobial Agents and Chemotherapy*, *60*(10), 6313–6325.

https://doi.org/10.1128/AAC.00830-16

Rajpaul, K. (2015). Biofilm in wound care. *British Journal of Community Nursing*, *20*(March), S6–S11. https://doi.org/10.12968/bjcn.2015.20.Sup3.S6

Reiber, G. E., Boyko, E. J., & Smith, D. G. (1995). Lower Extremity Foot Ulcers and Amputations in Diabetes. *Lower Extremity*, *2*(January), 409–428. http://ndic.circlesolutions.com/dm/pubs/america/pdf/chapter18.pdf

Rescignano, N., Tarpani, L., Romani, A., Bicchi, I., Mattioli, S., Emiliani, C., Torre, L., Kenny, J. M., Martino, S., Latterini, L., & Armentano, I. (2016). In-vitro degradation of PLGA nanoparticles in aqueous medium and in stem cell cultures by monitoring the cargo fluorescence spectrum. *Polymer Degradation and Stability*, *134*, 296–304. https://doi.org/10.1016/j.polymdegradstab.2016.10.017

Robson, M. C., Stenberg, B. D., & Heggers, J. P. (1990). Wound Healing Alterations Caused by Infection. *Clinics in Plastic Surgery*, *17*(3), 485–492.

Rodrigues, M., Kosaric, N., Bonham, C. A., & Gurtner, G. C. (2019). Wound healing: A cellular perspective. *Physiological Reviews*, *99*(1), 665–706. https://doi.org/10.1152/physrev.00067.2017

Roux, M. V., Jiménez, P., Martín-Luengo, M. Á., Dávalos, J. Z., Sun, Z., Hosmane, R. S., & Liebman, J. F. (1997). The Elusive Antiaromaticity of Maleimides and Maleic Anhydride: Enthalpies of Formation of N-Methylmaleimide, N-Methylsuccinimide, N-Methylphthalimide, and N-Benzoyl-N-methylbenzamide. *Journal of Organic Chemistry*, *62*(9), 2732–2737. https://doi.org/10.1021/jo9621985

Rutter, L. (2018). Identifying and managing wound infection in the community. *British Journal of Community Nursing*, *23*(2011), S6–S14. https://doi.org/10.12968/bjcn.2018.23.Sup3.S6

Saeedi, P., Petersohn, I., Salpea, P., Malanda, B., Karuranga, S., Unwin, N., Colagiuri, S., Guariguata, L., Motala, A. A., Ogurtsova, K., Shaw, J. E., Bright, D., & Williams, R. (2019). Global and regional diabetes prevalence estimates for 2019 and projections for 2030 and 2045: Results from the International Diabetes Federation Diabetes Atlas, 9th edition. *Diabetes Research and Clinical Practice*, *157*, 107843. https://doi.org/10.1016/j.diabres.2019.107843

Samuelsen, Ø., Haukland, H. H., Jenssen, H., Krämer, M., Sandvik, K., Ulvatne, H., & Vorland, L. H. (2005). Induced resistance to the antimicrobial peptide lactoferricin B in Staphylococcus aureus. *FEBS Letters*, *579*(16), 3421–3426. https://doi.org/10.1016/j.febslet.2005.05.017

Samuelsen, Ø., Haukland, H. H., Kahl, B. C., von Eiff, C., Proctor, R. A., Ulvatne, H., Sandvik, K., & Vorland, L. H. (2005). Staphylococcus aureus small colony variants are resistant to the antimicrobial peptide lactoferricin B. *Journal of Antimicrobial Chemotherapy*, *56*(6), 1126–1129. https://doi.org/10.1093/jac/dki385

Scanlon, E. (2005). Wound infection and colonisation. *Nursing Standard*, *19*(24). https://doi.org/10.7748/ns2005.02.19.24.57.c3812

Schultz, G. S., & Mast, B. A. (1998). Molecular analysis of the environment of healing and chronic wounds: Cytokines, proteases, and growth factors. *Wounds*, *10*(SUPPL. F).

Schultz, G. S., Sibbald, R. G., Falanga, V., Ayello, E. A., Dowsett, C., Harding, K., Romanelli, M., Stacey, M. C., Teot, L., & Vanscheidt, W. (2003). Wound bed preparation: a systematic approach to wound management. *WOUND REPAIR AND REGENERATION*, *March-Apri*. https://doi.org/10.12968/bjcn.2003.8.sup2.11554

Sen, C. K. (2019). Human Wounds and Its Burden: An Updated Compendium of Estimates. *Advances in Wound Care*, *8*(2), 39–48. https://doi.org/10.1089/wound.2019.0946

Severino, P., Silveira, E. F., Loureiro, K., Chaud, M. V., Antonini, D., Lancellotti, M., Sarmento, V.

H., da Silva, C. F., Santana, M. H. A., & Souto, E. B. (2017). Antimicrobial activity of polymyxin-loaded solid lipid nanoparticles (PLX-SLN): Characterization of physicochemical properties and in vitro efficacy. *European Journal of Pharmaceutical Sciences*, *106*, 177–184. https://doi.org/10.1016/j.ejps.2017.05.063

Shajari, G., Khorshidi, A., & Moosavi, G. (2017). Vancomycin resistance in Staphylococcus aureus strains. *Archives of Razi Institute*, *90*(54), 107–110.

Silhavy, T. J., Kahne, D., & Walker, S. (2010). The Bacterial Cell Envelope. *Cold Spring Harb Perspect Biol*, *2*, 1–16. https://www.ncbi.nlm.nih.gov/pmc/articles/PMC2857177/pdf/cshperspect-PRK-a000414.pdf

Silva, O. N., De La Fuente-Núñez, C., Haney, E. F., Fensterseifer, I. C. M., Ribeiro, S. M., Porto, W. F., Brown, P., Faria-Junior, C., Rezende, T. M. B., Moreno, S. E., Lu, T. K., Hancock, R. E. W., & Franco, O. L. (2016). An anti-infective synthetic peptide with dual antimicrobial and immunomodulatory activities. *Scientific Reports*, *6*, 1–11. https://doi.org/10.1038/srep35465

Singh, G., Kaur, T., Kaur, R., & Kaur, A. (2014). Recent biomedical applications and patents on biodegradable polymer-PLGA. *International Journal of Pharmacology and Pharmaceutical Sciences*, *1*(2), 30–42.

Subbalakshmi, C., Nagaraj, R., & Sitaram, N. (1999). Biological activities of C-terminal 15-residue synthetic fragment of melittin: Design of an analog with improved antibacterial activity. *FEBS Letters*, *448*(1), 62–66. https://doi.org/10.1016/S0014-5793(99)00328-2

Suk, J. S., Xu, Q., Kim, N., Hanes, J., & Ensign, L. M. (2017). PEGylation as a strategy for improving nanoparticle-based drug and gene delivery. *Advanced Drug Delivery Reviews*, *99*, 28–51. https://doi.org/10.1016/j.addr.2015.09.012.PEGylation

Sun, T., Zhan, B., Zhang, W., Qin, D., Xia, G., Zhang, H., Peng, M., Li, S. A., Zhang, Y., Gao, Y., & Lee, W. H. (2018). Carboxymethyl chitosan nanoparticles loaded with bioactive peptide OH-CATH30 benefit nonscar wound healing. *International Journal of Nanomedicine*, *13*, 5771–5786. https://doi.org/10.2147/IJN.S156206

Takeuchi, I., Suzuki, T., & Makino, K. (2017). Skin permeability and transdermal delivery route of 50-nm indomethacin-loaded PLGA nanoparticles. *Colloids and Surfaces B: Biointerfaces*, *159*, 312–317. https://doi.org/10.1016/j.colsurfb.2017.08.003

Thapa, R. K., Diep, D. B., & Tønnesen, H. H. (2020). Topical antimicrobial peptide formulations for wound healing: Current developments and future prospects. *Acta Biomaterialia*, *103*, 52–67. https://doi.org/10.1016/j.actbio.2019.12.025

Thapa, R. K., Winther-Larsen, H. C., Diep, D. B., & Tønnesen, H. H. (2020). Preformulation studies on novel garvicin KS peptides for topical applications. *European Journal of Pharmaceutical Sciences*, *151*(April), 105333. https://doi.org/10.1016/j.ejps.2020.105333

Tolker-Nielsen, T. I. M. (2015). Biofilm Development. *Microbiology Spectrum*, *3*(2), 1–12. https://doi.org/10.1128/microbiolspec

Tong, S. Y. C., Davis, J. S., Eichenberger, E., Holland, T. L., & Fowler, V. G. (2015). Staphylococcus aureus infections: Epidemiology, pathophysiology, clinical manifestations, and management. *Clinical Microbiology Reviews*, *28*(3), 603–661. https://doi.org/10.1128/CMR.00134-14

Toscano, W. A., & Storm, D. R. (1982). Bacitracin. *Pharmacology and Therapeutics*, *16*(2), 199–210. https://doi.org/10.1016/0163-7258(82)90054-7

Ulmschneider, J. P. (2017). Charged Antimicrobial Peptides Can Translocate across Membranes without Forming Channel-like Pores. *Biophysical Journal*, *113*(1), 73–81. https://doi.org/10.1016/j.bpj.2017.04.056

Umerska, A., Cassisa, V., Bastiat, G., Matougui, N., Nehme, H., Manero, F., Eveillard, M., &

Saulnier, P. (2017a). Synergistic interactions between antimicrobial peptides derived from plectasin and lipid nanocapsules containing monolaurin as a cosurfactant against Staphylococcus aureus. *International Journal of Nanomedicine*, *12*, 5687–5699.

van der Does, A. M., Hiemstra, P. S., & Mookherjee, N. (2019). Antimicrobial host defence peptides: Immunomodulatory functions and translational prospects. *Advances in Experimental Medicine and Biology*, *1117*, 149–171. https://doi.org/10.1007/978-981-13-3588-4_10

Vijayan, A., James, P. P., Nanditha, C. K., & Vinod Kumar, G. S. (2019). Multiple cargo deliveries of growth factors and antimicrobial peptide using biodegradable nanopolymer as a potential wound healing system. *International Journal of Nanomedicine*, *14*, 2253–2263. https://doi.org/10.2147/IJN.S190321

Viljanen, P., & Vaara, M. (1984). Susceptibility of gram-negative bacteria to polymyxin B nonapeptide. *Antimicrobial Agents and Chemotherapy*, *25*(6), 701–705. https://doi.org/10.1128/AAC.25.6.701

Wadhwani, P., Heidenreich, N., Podeyn, B., Bürck, J., & Ulrich, A. S. (2017). Antibiotic gold: Tethering of antimicrobial peptides to gold nanoparticles maintains conformational flexibility of peptides and improves trypsin susceptibility. *Biomaterials Science*, *5*(4), 817–827. https://doi.org/10.1039/c7bm00069c

Walshe, C. (1995). Living with a venous leg ulcer: a descriptive study of patients'experiences. In *Journal of Advanced Nursing* (Vol. 22, Issue 6, pp. 1092–1100). https://doi.org/10.1111/j.1365-2648.1995.tb03110.x

Walters, M. S., Eggers, P., Albrecht, V., Travis, T., Lonsway, D., Hovan, G., Taylor, D., Rasheed, K., Limbago, B., & Kallen, A. (2015). Vancomycin-Resistant Staphylococcus aureus — Delaware, 2015 . *MMWR. Morbidity and Mortality Weekly Report*, *64*(37), 1056. https://doi.org/10.15585/mmwr.mm6437a6

Wang, L., Hu, C., & Shao, L. (2017). The antimicrobial activity of nanoparticles: Present situation and prospects for the future. *International Journal of Nanomedicine*, *12*, 1227–1249. https://doi.org/10.2147/IJN.S121956

WHO. (2013). *Prevention and management of wound infection Guidance from WHO's Department of Violence and Injury Prevention and Disability and the Department of Essential Health Technologies*. https://www.who.int/hac/techguidance/tools/guidelines_prevention_and_management_wound_infection.pdf

WHO. (2017). *Global action plan on antimicrobial resistance*.

WHO. (2020). *Antimicrobial resistance*. https://www.who.int/news-room/fact-sheets/detail/antimicrobial-resistance

Wiegand, I., Hilpert, K., & Hancock, R. E. W. (2008). Agar and broth dilution methods to determine the minimal inhibitory concentration (MIC) of antimicrobial substances. *Nature Protocols*, *3*(2), 163–175. https://doi.org/10.1038/nprot.2007.521

Willyard, C. (2017). The drug-resistant bacteria that pose the greatest health threats. *Nature*, *543*(7643), 15. https://doi.org/10.1038/nature.2017.21550

Wu, X., Wei, P. H., Zhu, X., Wirth, M. J., Bhunia, A., & Narsimhan, G. (2017). Effect of immobilization on the antimicrobial activity of a cysteine-terminated antimicrobial Peptide Cecropin P1 tethered to silica nanoparticle against E. coli O157:H7 EDL933. *Colloids and Surfaces B: Biointerfaces*, *156*, 305–312. https://doi.org/10.1016/j.colsurfb.2017.05.047

Wu, Y. K., Cheng, N. C., & Cheng, C. M. (2019). Biofilms in Chronic Wounds: Pathogenesis and Diagnosis. *Trends in Biotechnology*, *37*(5), 505–517.

https://doi.org/10.1016/j.tibtech.2018.10.011

Xu, J., Li, Y., Wang, H., Zhu, M., Feng, W., & Liang, G. (2021). Enhanced antibacterial and anti-biofilm activities of antimicrobial peptides modified silver nanoparticles. *International Journal of Nanomedicine*, *16*, 4831–4846. https://doi.org/10.2147/IJN.S315839

Xu, Y., Kim, C. S., Saylor, D. M., & Koo, D. (2017). Polymer degradation and drug delivery in PLGA-based drug–polymer applications: A review of experiments and theories. *Journal of Biomedical Materials Research - Part B Applied Biomaterials*, *105*(6), 1692–1716. https://doi.org/10.1002/jbm.b.33648

Zasloff, M. (1987). Magainins, a class of antimicrobial peptides from Xenopus skin: Isolation, characterization of two active forms, and partial cDNA sequence of a precursor. *Proceedings of the National Academy of Sciences of the United States of America*, *84*(15), 5449–5453. https://doi.org/10.1073/pnas.84.15.5449

Zhao, R., Liang, H., Clarke, E., Jackson, C., & Xue, M. (2016). Inflammation in chronic wounds. *International Journal of Molecular Sciences*, *17*(12), 1–14. https://doi.org/10.3390/ijms17122085

Zhong, H., Chan, G., Hu, Y., Hu, H., & Ouyang, D. (2018). A comprehensive map of FDA-approved pharmaceutical products. *Pharmaceutics*, *10*(4), 1–19. https://doi.org/10.3390/pharmaceutics10040263